Supplementary information for: Ancient west Eurasian ancestry in southern and eastern Africa

Joseph K. Pickrell[1,7,†], Nick Patterson[2], Po-Ru Loh[3], Mark Lipson[3], Bonnie Berger[2,3], Mark Stoneking[4], Brigitte Pakendorf[5,†], David Reich[1,2,6,†]

[1] Department of Genetics, Harvard Medical School

[2] Broad Institute

[3] Department of Computer Science and Mathematics and AI Laboratory, MIT

[4] Department of Evolutionary Genetics, MPI for Evolutionary Anthropology

[5] Laboratoire Dynamique du Langage, UMR5596, CNRS and Université Lyon Lumière 2

[6] Howard Hughes Medical Institute, Harvard Medical School

[7] Current address: New York Genome Center

[†] To whom correspondence should be addressed: `jkpickrell@nygenome.org`, `brigitte.pakendorf@cnrs.fr`, `reich@genetics.med.harvard.edu`

January 12, 2014

Contents

1 Materials and Methods

1.1 Details of analyzed samples

1.1.1 Affymetrix data

The main southern African dataset in this paper is from Pickrell et al. [2012] (the dataset before filtering for outlier individuals). We genotyped an additional 32 samples from these populations on the Affymetrix Human Origins Array (Supplementary Table 1). As with the original dataset [Pickrell et al., 2012], these additional samples were obtained as part of a multidisciplinary project investigating the prehistory of the Khoisan peoples and languages (http://www2.hu-berlin.de/kba/) with prior informed written consent from all donors, and with ethical clearance from the Review Board of the University of Leipzig and with the permission of the Ministry of Youth, Sport and Culture of Botswana and the Ministry of Health and Social Services of Namibia. We then examined all populations in this merged dataset for outliers, and removed 17 individuals (Supplementary Figure 1).

We merged these data with those from Patterson et al. [2012] and Meyer et al. [2012], and all other samples genotyped on the same array. In analyses of multiple mixture events, we used a set of 51 populations (Supplementary Table 2). For most analyses of the Khoisan, we excluded the Damara because they appear genetically similar to Niger-Congo speakers [Pickrell et al., 2012]. These data consist of 565,259 SNPs; for most analyses, we use all of these SNPs. However, in some places (where noted) we used only subsets of these SNPs from known ascertainment panels. For analysis of multiple mixture dates we used the set of populations listed in Supplementary Table 2.

1.1.2 Illumina data

We merged data from several published sources [Altshuler et al., 2010; Behar et al., 2010; Henn et al., 2011; Li et al., 2008; Pagani et al., 2012; Schlebusch et al., 2012]. The merged dataset consisted of 2,935 individuals genotyped at 256,540 SNPs. For analyses of multiple mixture events, we used a set of 55 populations (Supplementary Table 7).

1.2 Estimating multiple dates of population mixture from weighted LD.

1.2.1 Theory

Here, we consider the properties of admixture LD in the presence of multiple admixture events in the history of a population. Consider two bi-allelic SNPs, x and y, in a haploid population T, and let the covariance between the genotypes (coded as 0 and 1 according to an arbitrary reference) be $z_T(x,y)$. This follows the notation in Loh et al. [2013]; note that $z_T(x,y)$ is simply the standard measure of LD often called D. The demographic history of population T influences $z_T(x,y)$ in a known fashion. First, if T derived from a single admixture event between two populations A and B with mixture proportions of α and $1-\alpha$, respectively, then t_1 generations after admixture in a population of infinite size [Chakraborty and Weiss, 1988]:

$$z_T(x,y) = [\alpha z_A(x,y) + (1-\alpha)z_B(x,y) + \alpha(1-\alpha)\delta_{AB}(x)\delta_{AB}(y)]e^{-t_1 d}, \tag{1}$$

where d is the genetic distance between x and y and $\delta_{AB}(x)$ is the difference in allele frequencies at SNP x between populations A and B. In Loh et al. [2013], it is assumed that $z_A(x,y) = z_B(x,y) = 0$. However, instead consider the case where population A itself is descended from admixture between populations C and

D at time t_2, with admixture fractions β and $1 - \beta$, respectively (Supplementary Figure 4). If $z_C(x, y) = z_D(x, y) = 0$ (i.e. neither C nor D is admixed), then:

$$z_T(x, y) = [\alpha\beta(1 - \beta)\delta_{CD}(x)\delta_{CD}(y)e^{-(t_2-t_1)d} + \alpha(1 - \alpha)\delta_{AB}(x)\delta_{AB}(y)]e^{-t_1 d} \tag{2}$$

$$= \alpha\beta(1 - \beta)\delta_{CD}(x)\delta_{CD}(y)e^{-t_2 d} + \alpha(1 - \alpha)\delta_{AB}(x)\delta_{AB}(y)e^{-t_1 d}. \tag{3}$$

If C or D is itself admixed, this simply adds another exponential term to $z_T(x, y)$. Generalizing to n population mixtures, we can see that

$$z_T(x, y) = \sum_{i=1}^{n} W_i \delta_i(x)\delta_i(y)e^{-t_i d}, \tag{4}$$

where $t_1, t_2, ..., t_n$ are the times of the various mixture events, W_i is a function of the mixture proportions of event i (and the contribution of this mixture event to T), and $\delta_i(x)$ is the difference in allele frequencies at locus x between the two populations involved in mixture event i.

Now, following Loh et al. [2013], consider two reference populations, A' and B'. We can now define a weighted measure of LD:

$$a_{A'B'}(x, y) = z_T(x, y)\delta_{A'B'}(x)\delta_{A'B'}(y) \tag{5}$$

$$= \sum_{i=1}^{n} W_i \delta_i(x)\delta_{A'B'}(x)\delta_i(y)\delta_{A'B'}(y)e^{-t_i d}. \tag{6}$$

If we then take the expected value of $a_{A'B'}$ at some genetic distance d:

$$E[a_{A'B'}(d)] = \sum_{i=1}^{n} W_i E[\delta_i \delta_{A'B'}]^2 e^{-t_i d}. \tag{7}$$

In the diploid case, all the entries here are simply multiplied by a factor of two [Loh et al., 2013].

1.2.2 Model fitting

Consider a set of m reference populations, $X_1, X_2, ..., X_m$, from which we have sampled $N_1, N_2, ..., N_m$ individuals, respectively, and genotyped L SNPs. Let there be a single target population T, and we have sampled N_T samples from this population. We can calculate the weighted LD statistic in population T using each pair of reference populations i and j:

$$\hat{a}_{ij}(d) = \frac{\sum_{\{x,y\}\in S(d)} \hat{z}_T(x, y)\hat{\delta}_{ij}(x)\hat{\delta}_{ij}(y)}{|S(d)|}, \tag{8}$$

where $\hat{\delta}_{ij}(x) = \hat{f}_i(x) - \hat{f}_j(x)$, $\hat{f}_i(x)$ is the trivial estimator of the allele frequency at locus x in population i, $S(d)$ is the set of all pairs of SNPs separated by genetic distance d, and

$$\hat{z}_T(x, y) = \frac{1}{N_T - 1}\sum_{k=1}^{N_T}(g_{kx} - \bar{g}_x)(g_{ky} - \bar{g}_y), \tag{9}$$

where g_{kx} is the genotype of individual k in population T at locus x (coded as 0, 1, or 2 copies of an

3

arbitrarily defined reference allele), and $\bar{g}_x = \frac{1}{N_T} \sum_k g_{kx}$.

For a given target population, then, we can calculate $\binom{m}{2}$ curves of weighted LD (in practice, we can do this extremely quickly using the algorithm in Loh et al. [2013]). The theory above tells us that each curve is a mixture of exponential curves. We thus model each curve as:

$$\hat{a}_{ij}(d) = K_{ij} + \sum_{k=1}^{n} C_{ijk} e^{-t_k d} + \epsilon_{ij}(d),$$ (10)

where K_{ij} is an affine term estimated for each pair of populations, C_{ijk} is the amplitude of the kth exponential term for populations i and j, $\epsilon_{ij}(d)$ are error terms distributed as $N(0, \sigma_{ij}^2)$ (note that these error terms are not independently distributed, so we will use a jackknife to judge fit), and t_k is the time of the kth admixture event. *The key fact is that different pairs of reference populations often have different relative values of C_{ij} but always have fixed values of t.* This in principle gives us some leverage in the tricky problem of fitting mixtures of exponentials.

We now want to estimate all the parameters in Equation 10. These include the number of waves of mixture, the amplitudes, and the admixture times. We treat this as a least squares problem; that is, we want to minimize $\sum_{ij} (\hat{a}_{ij}(d) - E[a_{ij}(d)])^2$. We start by assuming a single wave of admixture. For a fixed time, the amplitudes can be solved by non-negative least squares. We then numerically optimize the admixture times (also enforcing non-negativity) using the Nelder-Mead algorithm implemented in the GNU scientific library [Galassi et al., 2002]. Once the model is fit, we calculate jackknife standard errors of all the parameters, by dropping each chromosome in turn and re-optimizing. In all cases, we started fitting curves only from 0.5 cM. If the curve is "significant" we add another exponential term. In total, the algorithm is:

1. Add a new exponential term to the model.

2. Fit the model by alternately optimizing all exponential decay terms and amplitudes.

3. Calculate standard errors on all terms using a jackknife.

4. If all decay terms have a p-value less than 0.01, go back to step 1, otherwise finish.

In this model, each pair of populations is treated as independent. We thus additionally experimented with performing a bootstrap where we randomly sample pairs of populations rather than re-sampling chromosomes. The results from this analysis were qualitatively similar to those presented, so we use the standard errors from the above jackknife procedure.

To infer the sources of admixture for each admixture time, we examined the C_{ijk} parameters (recall that these are the amplitudes of the LD curve computed using populations i and j on the admixture time k). For each Khoisan population, we identified the maximum C_{ijk} where i or j was a Niger-Congo-speaking group and the other was a Khoisan group. Call this C_{NC}^{max}. We then identified the maximum C_{ijk} where either i or j was a west Eurasian group and the other was a Khoisan group. Call this C_{WE}^{max}. We also have the standard errors on these estimates from the jackknife. We then computed a Z-score to test whether these were significantly different:

$$Z = \frac{C_{NC}^{max} - C_{WE}^{max}}{\sqrt{se(C_{NC}^{max})^2 + se(C_{WE}^{max})^2}}.$$ (11)

If the p-value from this test was greater than 0.05, in Figure 4 in the main we show this as a low-confidence ancestry call.

To compare the amplitudes in the eastern African populations, we performed the same type of test. The exact same test is not possible because we have no set of populations in eastern Africa that are analogous to

the Khoisan in southern Africa in representing presumably autochthonous groups. Instead, we compared the set of C_{ijk} where one reference population was Eurasian to the set of C_{ijk} where neither reference population was Eurasian. We separately compared the set of C_{ijk} where one population was a Niger-Congo-speaking agriculturalist group to the set of C_{ijk} where neither population was a Niger-Congo-speaking agriculturalist group. We then report the relevant Z-score (that is, if the overall maximum C_{ijk} included a Eurasian population, we reported the first Z-score, while if the overall maximum C_{ijk} included a Niger-Congo-speaking agriculturalist group, we reported the second Z-score. In the cases where the overall maximum C_{ijk} included both a Eurasian population and a Niger-Congo-speaking population, we reported the minimum of the two Z-scores).

1.2.3 Conditions under which the mixture weights do not identify the true admixing populations.

When fitting the above model, for a given pair of populations i and j on admixture event k, we estimate a parameter C_{ijk}. The relative values of these parameters for different populations reflect the differential relationships of i and j to the true admixing populations. We asked in what situation the maximum values of these parameters do not identify the reference populations most closely related to the true admixing populations.

Consider the two-admixture situation presented in Supplementary Figure 4, and let the earliest admixture event (between populations C and D) be too old to detect by LD, and so the only curve in the data has a decay rate of t_2 generations. Now consider the LD curve computed using populations A and B as references (these are the true admixing populations) and that computed using B and C as references. The two curves have the form:

$$E[a_{AB}(d)] = \alpha(1-\alpha)E[\delta_{AB}\delta_{AB}]^2 e^{-t_2 d} \tag{12}$$

$$E[a_{CB}(d)] = \alpha(1-\alpha)E[\delta_{AB}\delta_{CB}]^2 e^{-t_2 d}, \tag{13}$$

$$\tag{14}$$

so the curve computed using the true mixing populations will have the highest amplitude when $E[\delta_{AB}\delta_{AB}]^2 > E[\delta_{AB}\delta_{CB}]^2$. Writing these out explicitly (using the branch lengths in Supplementary Figure 4),

$$E[\delta_{AB}\delta_{AB}] = x_1 + x_2 + \beta^2 x_3 + (1-\beta)^2 x_4 + x_5 \tag{15}$$

$$E[\delta_{CB}\delta_{AB}] = x_1 + x_2 + \beta x_3. \tag{16}$$

Thus, weighted LD curves computed using the true mixing populations have the highest amplitude when $\beta^2 x_3 + (1-\beta)^2 x_4 + x_5 > \beta x_3$. Note that x_3 is weighted by β^2 on the left hand side and β on the right hand side. In our applications, European populations correspond to population C, β corresponds to the amount of west Eurasian ancestry, and the branch x_3 corresponds to the out-of-Africa bottleneck, which induced a large amount of genetic drift. We thus expect the amplitude to be dominated by the x_3 term, and to identify a Eurasian population as the best reference population if the true source population has even a low level of Eurasian admixture.

1.2.4   Simulations

To test the performance of our approach to estimate multiple mixture dates, we used coalescent simulations implemented in the software macs [Chen et al., 2009]. The basic simulation setup is shown in Supplementary Figure 5. For each simulation, we simulated 30 individuals from each of the nine populations, and each individual consisted of 10 independent chromosomes of 200Mb. We thus simulated many aspects of real data, including hundreds of thousands of SNPs in linkage disequilibrium. We simulated three scenarios: $t_1 = 20$ and $t_2 = 100$, $t_1 = 20$ and $t_2 = 60$, and $t_1 = 40$ and $t_2 = 100$. We additionally performed simulations of scenarios with a single episode of population mixture (at times of either 20 generations in the past or 100 generations in the past). The exact macs command used was (for, e.g., $t_1 = 40$ and $t_2 = 100$):

```
macs 540 200000000 -t 0.00004 -r 0.0004 -I 9 60 60 60 60 60 60 60 60 60 0 -em 0.0010 1 4
8000 -em 0.001025 1 4 0 -em 0.0025 1 7 8000 -em 0.002525 1 7 0 -ej 0.0125 7 8 -ej 0.0125 1
2 -ej 0.0125 4 5 -en 0.0249 8 0.02 -ej 0.025 8 9 -en 0.0249 2 0.02 -ej 0.025 2 3 -en 0.0249
5 0.02 -ej 0.025 5 6 -en 0.0748 9 0.01 -ej 0.075 6 9 -en 0.1498 9 0.01 -ej 0.15 3 9
```

Each simulation consisted of 10 replicates of the above command. We then ran our method to identify multiple mixture dates on the admixed population using all eight other simulated populations as references. Results are shown in Supplementary Figure 6. In the case with a large difference in the mixture times ($t_1 = 20$ and $t_2 = 100$), the method behaves well in all simulations. In harder cases (when either the mixture times are close together or both are old), the method occasionally misses the second mixture event or results in extremely large confidence intervals. Additionally, in two simulations where the method identifies the correct number of admixture events, the confidence intervals on the dates do not overlap the true values. Overall, however, in 18/20 such simulations (where the method identifies the correct number of admixture events), the 95% confidence intervals include the true values.

To gain some intuition into the performance of the model, we examined the LD curves underlying the fitted models. In Supplementary Figure 8, we show an example fitted model under the simulation where $t_1 = 20$ and $t_2 = 100$, and in Supplementary Figure 9 we show the same plot for a simulation where $t_1 = 40$ and $t_2 = 100$. The reason for the change in performance is clear: when both admixture events are older, the fit of the single exponential curve is already reasonably good and adding a second exponential in this case only marginally (though significantly in this case) improves the fit. However, when one of the admixture events is more recent, the fit of the single exponential curve becomes visibly poor.

We additionally simulated a situation with a low level of gene flow from population 4 into population 1 over the course of 100 generations (rather than in a single pulse, as assumed in the model). The exact macs command used for this simulation was:

```
macs 540 200000000 -t 0.00004 -r 0.0004 -I 9 60 60 60 60 60 60 60 60 60 0 -em 0.0005 1 4
80 -em 0.003 1 4 0 -ej 0.0125 7 8 -ej 0.0125 1 2 -ej 0.0125 4 5 -en 0.0249 8 0.02 -ej 0.025
8 9 -en 0.0249 2 0.02 -ej 0.025 2 3 -en 0.0249 5 0.02 -ej 0.025 5 6 -en 0.0748 9 0.01 -ej 0.075
6 9 -en 0.1498 9 0.01 -ej 0.15 3 9
```

Again, each simulation consisted of 10 replicates of the above command, and applied our model. In this situation, the model sometimes infers that this represents two pulses of admixture from the same source (Supplementary Figure 7). In applications to real data, we sometimes infer two pulses of admixture from the same source (e.g. in the Nama and Taa_West in southern Africa, and the Oromo, Maasai, Amhara, and Gumuz in eastern Africa); in these cases, a potential alternative interpretation is low level gene flow over a long period of time rather then two discrete pulses of gene flow.

An additional source of error for methods like this are demographic complexities like population bottlenecks. Loh et al. [2013] show that a shared bottleneck in the history of one of the reference populations and a

test population can generate a curve of weighted LD that mimics that of admixture to some degree. However, the amplitudes of bottleneck-induced weighted LD curves do not depend on the reference populations used [Loh et al., 2013], so we do not consider this further in our analyses of southern Africa.

1.3   Analysis of combined populations

In most southern African populations where our method detects only a single admixture event, the fitted model visually appears inadequate to fully explain the data (e.g. Supplementary Figures 10, 12, 17, 20). Indeed, there is marginal statistical evidence for two admixture events in many of these populations (Supplementary Table 3). As described in the main text, we performed analyses of combined populations. Note that combining populations induces LD across the whole genome, but does not induce a decay curve; if populations share an admixture event, combining the populations should result in increased power to detect it.

We first combined a set of populations (the Tshwa, Shua, Hai||om, ǂHoan, Naro, and Taa_North) that appear to have weak evidence for a second, more recent admixture event (Supplementary Table 3), and ran our method on this combined sample. In this combined sample we infer two dates of admixture: one 40 ± 2 generations ago and one 4 ± 1 generations ago (Z-score of 3.2, $P = 7 \times 10^{-4}$), with the more recent admixture involving Bantu-speaking populations, though this ancestry assignment is made with low confidence.

We then combined two populations (the Ju|'hoan_North and G|ui) that have weak evidence for a second, more ancient admixture event (Supplementary Table 3). In this combined sample (Supplementary Figure 23), we also infer two dates of admixture, but with different dates from all other samples: one 30 ± 4 generations ago, and one 109 ± 41 generations ago (Z-score of 2.6, $P = 0.005$). We interpret this as evidence that the population that introduced west Eurasian ancestry to southern Africa was itself admixed, and that this more ancient admixture happened around 110 generations ago (though the confidence intervals here are clearly large). However, we cannot exclude the possibility that the Ju|'hoan_North and G|ui alone experienced gene flow from this admixed population, while the west Eurasian ancestry detected in the other southern African populations stems from a different population that did not carry this signal of ancient admixture.

1.4 f_4 ancestry estimation.

To estimate the fraction of west Eurasian ancestry in each African population, we used the fact that this ancestry appears to be more closely related to southern Europe and the Middle East than to northern Europe. We thus computed the f_4 ratio f_4(Han, Orcadian; X, Druze) / f_4(Han, Orcadian; Yoruba, Druze), where X is any African population. (Supplementary Figure 40). Since the Druze have a small level of west African ancestry, this ratio is not exactly the desired fraction. Instead, if we let λ be the fraction of Druze-like ancestry in population X and F be the fraction of Yoruba-like ancestry in the Druze:

$$\frac{f_4(H, O; X, D)}{f_4(H, O; Y, D)} = \frac{1 - \lambda - F}{1 - F}. \tag{17}$$

We approximate λ by assuming $F = 0.05$ for the Druze [Moorjani et al., 2011]. In some cases, our estimates of west Eurasian ancestry are slightly below zero (though not statistically significantly so); for these populations we report the ancestry proportion as 0%.

1.5 Estimating the allele frequencies of the west Eurasian population that admixed into eastern Africa.

We sought to impute the allele frequencies of the ancestral west Eurasian population that entered eastern Africa. To do this, we model the allele frequencies in a set of N eastern African populations as a weighted combination of allele frequencies in the Sudanese (we choose the Sudanese because they are often the best proxy for the African ancestry in Ethiopian populations; Supplementary Table 4) and an unknown west Eurasian population. Let $\hat{f}_S$ be the estimated allele frequency at a given SNP in the Sudanese, f_X be the (unknown) allele frequency at the SNP in the ancestral west Eurasian population, and f_j be the population allele frequency (as opposed to the sample allele frequency) of the SNP in eastern African population j. We model f_j as:

$$f_j = f_X \hat{w}_X + \hat{f}_S \hat{w}_S, \tag{18}$$

where $\hat{w}_X$ is the estimated proportion of west Eurasian ancestry in population j from Table 1 in the main text and $\hat{w}_S = 1 - \hat{w}_X$. For a given f_X, the sum of squared errors is:

$$SS(f_X) = \sum_{j=1}^{N} (\hat{f}_j - f_j)^2, \tag{19}$$

where $\hat{f}_j$ is the estimated allele frequency at the SNP in population j. We then search over values of f_X to minimize Equation 19.

In the set of east African populations, we included the six with the most west Eurasian ancestry: the Tygray, Amhara, Afar, Oromo, Somali, and Ethiopian Somali. We then minimized Equation 19 for each SNP in the Illumina data using the optimize() function in R [R Development Core Team, 2011]. To compare to an ancestral Middle Eastern population, we performed the same analysis on the Bedouin, Druze, and Palestinian populations, using the estimated African ancestry proportions from Moorjani et al. [2011].

To run ALDER using these imputed allele frequencies, we calculated the ALDER weighted LD statistic in the Juhoansi (since the eastern African populations were typed on an Illumina array, these are the samples from Schlebusch et al. [2012]) using weights calculated from the Juhoansi as one reference and the imputed allele frequencies as the other reference. To account for sampling error, we simulated 40 individuals from the inferred ancestral west Eurasian population using the estimated allele frequencies.

1.6 Partitioning non-Khoisan ancestry into putative eastern African and putative Bantu-related ancestry.

To partition the ancestry of all southern African groups into Khoisan, putative eastern African, and putative Bantu-related ancestry, we model the allele frequency at a given SNP in a Khoisan population f_X as a linear combination of the allele frequencies in the Ju|'hoan_North (f_J), Yoruba (f_Y), Dinka (f_D), and Italian (f_I):

$$f_X = w_1 f_J + w_2 f_Y + w_3 f_D + w_4 f_I, \tag{20}$$

where $\sum_{i=1}^{4} w_i = 1$. Using all SNPs, we estimated these weights using the approach of Patterson et al. [2010], using the Han as an outgroup population. If these four populations were the true unadmixed reference populations, these weights would correspond to the mixture fractions in population X. Since the Ju|'hoan_North are admixed and the Dinka may not be the best reference for an ancestral east African population, we took the following approach to convert these weights to the admixture fractions we are interested in: First, define

the proportion of west Eurasian ancestry as $w_E = 0.01w_1 + w_4$ and the proportion of Khoisan ancestry as $w_K = 0.96w_1$. We then computed the proportion of putative east African ancestry as $w_{EA} = 4w_E$ and the proportion of putative Bantu-related ancestry as $w_B = 1 - w_K - w_{EA}$.

2 Supplementary Tables

Population	# individuals
Taa_East	3
Taa_North	5
Taa_West	9
G|ui	6
G||ana	4
!Xuun	3
Nama	2

Table 1: **Additional southern African samples typed in this study.**

Population	# individuals
Adygei	15
Balochi	21
BantuKenya	10
BantuSouthAfrica	6
Basque	20
Bedouin	38
BiakaPygmy	20
Melanesian	9
Dai	10
Damara	13
Dinka	7
Druze	32
Taa_East	8
French	26
G‖ana	7
G∣ui	7
Hadza	24
Hai‖om	9
Himba	5
Han	32
ǂHoan	7
Italian	11
Japanese	28
Ju∣'hoan_North	21
Ju∣'hoan_South	6
Kalash	18
Khwe	10
Tshwa	9
Mandenka	20
Mbukushu	5
MbutiPygmy	11
Mozabite	25
Nama	18
Naro	9
Taa_North	9
Orcadian	13
Wambo	5
Palestinian	34
Russian	22
Sardinian	26
Shua	9
Tswana	5
Tuscan	7
Taa_West	16
!Xuun	13
Yoruba	21

Table 2: **Populations typed on the Affymetrix Human Origins array used in analyses of multiple mixture events.**

Population	Mixture date in generations	Best west African amplitude (populations)	Best Eurasian amplitude (populations)	Z-score (P)
ǂHoan	14	$3.2 \times 10^{-4} \pm 2.3 \times 10^{-5}$ (Taa_North; Yoruba)	$3.5 \times 10^{-4} \pm 2.8 \times 10^{-5}$ (Taa_North; Druze)	0.87 (0.38)
Tshwa	23	$3.6 \times 10^{-4} \pm 2.0 \times 10^{-5}$ (Ju|'hoan_South; Yoruba)	$4.3 \times 10^{-4} \pm 2.6 \times 10^{-5}$ (Italian;Ju|'hoan_South)	2.02 (0.04)
Taa_West	62	$1.4 \times 10^{-4} \pm 2.2 \times 10^{-5}$ (Ju|'hoan_South; BantuKenya)	$2.9 \times 10^{-4} \pm 2.5 \times 10^{-5}$ (Sardinian;Ju|'hoan_South)	4.6 (4×10^{-6})
Taa_West	8	$1.3 \times 10^{-4} \pm 2.6 \times 10^{-5}$ (Taa_North;Yoruba)	$1.4 \times 10^{-4} \pm 2.5 \times 10^{-5}$ (Taa_North;Kalash)	0.04 (0.97)
Taa_North	30	$2.5 \times 10^{-4} \pm 1.4 \times 10^{-5}$ (Taa_West;Yoruba)	$3.9 \times 10^{-4} \pm 2.5 \times 10^{-5}$ (Taa_West;Druze)	5.2 (2×10^{-7})
Taa_East	28	$3.0 \times 10^{-4} \pm 1.9 \times 10^{-5}$ (Taa_North;Yoruba)	$3.8 \times 10^{-4} \pm 1.4 \times 10^{-5}$ (Taa_West;Italian)	3.5 (5×10^{-4})
Taa_East	28	$8.2 \times 10^{-5} \pm 1.4 \times 10^{-5}$ (G|ui;Yoruba)	$7.1 \times 10^{-5} \pm 1.2 \times 10^{-5}$ (Bedouin;G|ui)	0.65 (0.52)
Shua	32	$3.8 \times 10^{-4} \pm 1.6 \times 10^{-5}$ (Ju|'hoan_South;Yoruba)	$4.5 \times 10^{-4} \pm 2.2 \times 10^{-5}$ (Ju|'hoan_South;Druze)	2.7 (0.007)
Naro	37	$2.4 \times 10^{-4} \pm 1.4 \times 10^{-5}$ (Ju|'hoan_South;BantuKenya)	$4.9 \times 10^{-4} \pm 2.8 \times 10^{-5}$ (Ju|'hoan_South;Sardinian)	7.8 (6×10^{-15})
Nama	5	$1.2 \times 10^{-4} \pm 1.3 \times 10^{-5}$ (Taa_West;Damara)	$4.1 \times 10^{-4} \pm 4.1 \times 10^{-5}$ (Taa_West;Orcadian)	6.6 (4×10^{-11})
Nama	55	$2.6 \times 10^{-4} \pm 1.7 \times 10^{-5}$ (Taa_West;BantuKenya)	$6.5 \times 10^{-4} \pm 5.5 \times 10^{-5}$ (Taa_West;Sardinian)	6.9 (5×10^{-12})
Khwe	60	$2.0 \times 10^{-4} \pm 1.1 \times 10^{-4}$ (Ju|'hoan_South;Yoruba)	$4.5 \times 10^{-4} \pm 7.1 \times 10^{-5}$ (Ju|'hoan_North;Tuscan)	2.0 (0.05)
Khwe	17	$1.7 \times 10^{-4} \pm 8.8 \times 10^{-5}$ (Ju|'hoan_North;Yoruba)	$1.4 \times 10^{-4} \pm 7.9 \times 10^{-5}$ (Ju|'hoan_North;Dai)	0.3 (0.76)
Ju|'hoan_South	39	$2.1 \times 10^{-4} \pm 3.1 \times 10^{-5}$ (Ju|'hoan_North;Mandenka)	$3.3 \times 10^{-4} \pm 9.4 \times 10^{-5}$ (Ju|'hoan_North;Dai)	1.3 (0.19)
Ju|'hoan_South	64	$5.6 \times 10^{-5} \pm 1.2 \times 10^{-5}$ (G||ana,Mbukushu)	$1.2 \times 10^{-4} \pm 4.1 \times 10^{-5}$ (G||ana;Italian)	3.3 (0.001)
Ju|'hoan_North	46	$2.3 \times 10^{-4} \pm 8.3 \times 10^{-6}$ (Ju|'hoan_South;Mandenka)	$4.1 \times 10^{-4} \pm 1.5 \times 10^{-5}$ (Ju|'hoan_South;Sardinian)	10.3 ($< 1 \times 10^{-15}$)
Hai||om	34	$4.3 \times 10^{-4} \pm 1.6 \times 10^{-5}$ (Ju|'hoan_North;Yoruba)	$6.2 \times 10^{-4} \pm 2.5 \times 10^{-5}$ (Ju|'hoan_North;Sardinian)	6.3 (3×10^{-10})
G|ui	31	$2.6 \times 10^{-4} \pm 1.3 \times 10^{-5}$ (Taa_North;Yoruba)	$4.3 \times 10^{-4} \pm 2.3 \times 10^{-5}$ (Taa_North;Sardinian)	6.5 (8×10^{-11})
G||ana	39	$3.0 \times 10^{-4} \pm 4.3 \times 10^{-5}$ (G|ui;Yoruba)	$4.1 \times 10^{-4} \pm 2.5 \times 10^{-5}$ (Taa_West;Italian)	2.3 (0.02)
G||ana	4	$1.4 \times 10^{-4} \pm 3.5 \times 10^{-5}$ (G|ui;Yoruba)	$1.1 \times 10^{-4} \pm 3.0 \times 10^{-5}$ (G|ui;Kalash)	0.5 (0.6)
!Xuun	43	$3.2 \times 10^{-4} \pm 2.2 \times 10^{-5}$ (Ju|'hoan_South;Yoruba)	$4.8 \times 10^{-4} \pm 2.2 \times 10^{-5}$ (Ju|'hoan_North;Sardinian)	5.1 (3×10^{-7})
!Xuun	4	$8.3 \times 10^{-5} \pm 1.4 \times 10^{-5}$ (Ju|'hoan_North;Yoruba)	$8.0 \times 10^{-5} \pm 1.4 \times 10^{-5}$ (Ju|'hoan_North;Druze)	0.11 (0.9)

Table 3: **Amplitudes of fitted admixture models for all southern African populations.** For each admixture event shown in Figure 4 in the main text in southern African populations, we show the amplitudes of the best "west African" populations (we include all Niger-Congo-speaking agriculturalist populations here, regardless of their geographic location) and "Eurasian" populations, and show the Z-score and corresponding P-value for a difference between the two.

Population	One-admixture model date (gen. before present)	One-admixture model Z-score (P-value)	Two-admixture model dates (gen. before present)	Two-admixture model Z-scores (P-values)
G|ui	31	11.9 (6×10^{-33})	109, 24	2.2 (0.014), 6.1 (5×10^{-10})
Hai||om	34	15.9 (3×10^{-57})	51, 13	1.8 (0.035), 0.55 (0.29)
Ju|'hoan_North	46	18.8 (4×10^{-79})	140, 38	1.7 (0.04), 8.4 (2×10^{-17})
Naro	37	11.4 (2×10^{-30})	43, 6	8.3 (5×10^{-17}), 1.8 (0.04)
Shua	32	14.0(8×10^{-45})	55, 18	1.9 (0.03), 1.8 (0.04)
Taa_North	30	10.4 (1×10^{-25})	44, 6	8.1 (3×10^{-16}), 1.9 (0.03)
Tshwa	23	10.1(3×10^{-24})	45, 6	8.0 (6×10^{-16}), 2.0 (0.02)
‡Hoan	14	7.1(6×10^{-13})	32, 6	3.1 (0.001), 1.8 (0.04)

Table 4: **Southern African populations with a single inferred admixture event.** For each southern African population where Figure 4 in the main text shows a single admixture event, we show the admixture times inferred from both the one- and two-admixture models. Additionally shown are the Z-scores and P-values for each admixture time (we used a P-value threshold of 0.01 to call an admixture event as "significant", so for all of these populations at least one mixture time in the two-admixture model is non-significant). The G\|ui and Ju\|'hoan_North stand out as having borderline evidence for an old admixture event around 100 generations ago.

Target Population	Reference populations	f_3	Z-score
Afar	Sardinian, Sudanese	-0.026	-66.4
Afar	Sardinian, Anuak	-0.026	-63.8
Afar	French Basque, Sudanese	-0.025	-61.0
Amhara	Tuscan, Sudanese	-0.028	-91.4
Amhara	Tuscan, Anuak	-0.028	-90.7
Amhara	Samaritans, Anuak	-0.027	-85.8
Anuak	Ari Blacksmith, Sudanese	-0.001	-8.2
Anuak	Ari Cultivator, Sudanese	-0.001	-8.6
Anuak	Wolayta, Sudanese	-0.001	-5.5
Ari Cultivator	Sardinian, Ju|'hoan	-0.013	-25.7
Ari Cultivator	Samaritian, Ju|'hoan	-0.013	-21.1
Ari Cultivator	Tuscan, Ju|'hoan	-0.013	-24.1
Ethiopian Somali	Sardinian, Sudanese	-0.024	-64.2
Ethiopian Somali	Sardinian, Anuak	-0.024	-64.1
Ethiopian Somali	Cypriot, Sudanese	-0.023	-64.2
Luhya	Sardinian, Biaka	-0.005	-16.8
Luhya	Bedouin, Biaka	-0.005	-17.4
Luhya	Yemenite Jews, Biaka	-0.005	-17.4
Maasai	Sardinian, Mbuti	-0.021	-54.5
Maasai	Cypriot, Mbuti	-0.021	-54.6
Maasai	Samaritian, Mbuti	-0.021	-42.8
Oromo	Sardinian, Sudanese	-0.031	-95.7
Oromo	Sardinian, Anuak	-0.030	-93.2
Oromo	Samaritian, Anuak	-0.030	-70.2
Somali	Sardinian, Sudanese	-0.022	-60.3
Somali	Sardinian, Anuak	-0.022	-60.5
Somali	French Basque, Sudanese	-0.021	-55.3
Tygray	Sardinian, Sudanese	-0.029	-88.7
Tygray	Sardinian, Anuak	-0.029	-87.2
Tygray	Cypriot, Sudanese	-0.028	-88.2
Wolayta	Sardinian, Gumuz	-0.025	-69.6
Wolayta	Cypriot, Gumuz	-0.024	-69.3
Wolayta	Yemenite Jews, Gumuz	-0.024	-72.0

Table 5: **Three-population tests for treeness in eastern Africa.** We performed three-population tests on all eastern African populations from Pagani et al. [2012] and the HapMap 3. For each population with at least one f_3 statistic with a Z-score less than -3, we show details of the three smallest f_3 statistics: the names of the reference populations, the value of the statistic, and the Z-score. A Z-score of less than -3 corresponds to a p-value of less than 0.001. The eastern African populations with no significantly negative f_3 statistics are the Sudanese, Gumuz, and Ari Blacksmith

Population	Mixture date in generations	Z-score (Eurasian versus non-Eurasian)	Z-score (west African versus non-west African)
Wolayta	59	6.5	1.0
Tygray	88	12.7	0.9
Somali	109	8.6	0.7
Sandawe	130	7.0	2.4
Sandawe	130	7.0	2.4
Sandawe	27	1.2	0.2
Oromo	95	12.9	1.0
Oromo	8	2.2	0.6
Maasai	88	22.5	1.1
Maasai	8	3.1	0.1
Luhya	106	4.6	0.8
Luhya	16	1.0	0.3
Hadza	61	3.2	0.5
Gumuz	5	5.1	0.6
Gumuz	112	2.3	0.6
ESomali	107	9.3	0.6
AriCultivator	104	7.2	1.5
AriBlacksmith	109	6.9	1.2
Anuanak	82	0.9	0.4
Amhara	115	14.2	1.5
Amhara	11	2.3	0.8
Afar	81	7.7	0.9

Table 6: **Amplitudes of fitted admixture models for all eastern African populations.** We split the reference populations used to calculate weighted LD in each population into "west African" (including all Niger-Congo-speaking agriculturalist populations), "Eurasian", and "other African" (including populations from southern and eastern Africa). We computed a Z-score comparing the largest amplitude where one reference population is Eurasian to the largest amplitude where neither population is Eurasian, as well as a Z-score comparing the largest amplitude where one reference population is west African to the largest amplitude where neither population is west African. Highlighted in grey is the comparison involving the overall maximum amplitude and thus the source population reported in Figure 4.

Population	# individuals
AMHARA	26
Khwe	17
Adygei	17
AFAR	12
ANUAK	23
ARIBLACKSMITH	17
ARICULTIVATOR	24
Armenians	19
BantuKenya	11
BantuSouthAfrica	8
Basque	24
Bedouin	45
BiakaPygmy	22
CEU (Utah)	112
Cypriots	12
Druze	42
Egyptians	12
ESOMALI	17
Ethiopians	19
Han	34
Japanese	28
French	28
Georgians	20
GuiGhanaKgal	15
GUMUZ	19
HADZA	17
Hungarians	20
Iranians	20
Italian	12
Jordanians	20
Juhoansi	23
Kalash	23
Khomani	39
Lebanese	8
LWK (Luhya)	90
Mandenka	22
MbutiPygmy	13
MKK (Maasai)	143
Moroccans	10
Mozabite	27
Nama	20
Orcadian	15
OROMO	21
Palestinian	46
Russian	25
SANDAWE	28
Sardinian	28
SOMALI	23
SUDANESE	24
Syrians	16
TSI (Tuscany)	88
TYGRAY	21
WOLAYTA	8
Xun	19
YRI (Yoruba)	113

Table 7: **Populations typed on an Illumina array and used in analyses of multiple mixture events.** Labels are taken from the papers in which the samples were first reported.

Table 8: **Estimates of the proportion of Khoisan, putative eastern African, and putative Bantu-related ancestry in southern African populations, ordered by the amount of putative eastern African ancestry.** The Nama were excluded from this analysis because of their recent European ancestry. Additionally shown is the proportion of west Eurasian ancestry in each population as estimated by the linear model (these proportions are slightly different from those in Table 1 in the main text).*The admixture proportions of the Ju|'hoan_North were fixed in this analysis.

Population	Khoisan ancestry (%)	Putative eastern African (west Eurasian) ancestry (%)	Putative Bantu-related ancestry (%)
Hai‖om	54	25 (6.3)	21
Shua	37	21 (5.2)	43
Khwe	36	18 (4.6)	45
G|ui	80	13 (3.2)	6
Tshwa	48	10 (2.4)	43
!Xuun	73	9 (2.2)	18
Naro	87	9 (2.2)	5
Taa_North	84	9 (2.4)	7
G‖ana	53	6 (1.5)	41
ǂHoan	70	6 (1.4)	24
Ju|'hoan_South	93	6 (1.5)	1
Damara	9	4 (1.0)	88
Ju|'hoan_North*	96	4 (1.0)	0
Mbukushu	9	2 (0.5)	89
Taa_East	74	1 (0.2)	25
Taa_West	83	1 (0.3)	16
Himba	8	0 (0)	92
Tswana	22	0 (0)	78
Kgalagadi	33	0 (0)	67
Wambo	5	0 (0)	95

3   Supplementary Figures
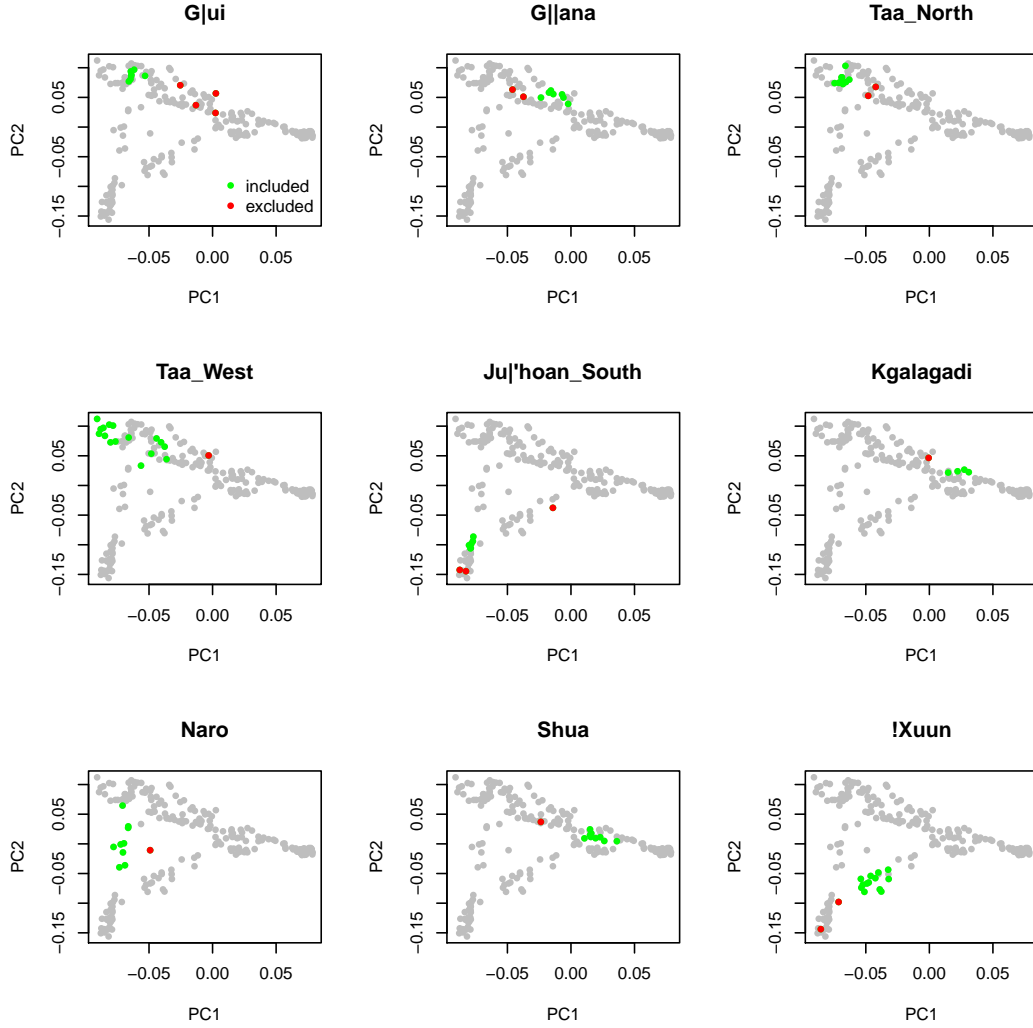
Figure 1: **Outliers in southern African data.** We ran smartpca [Patterson et al., 2006] on the southern African samples, and visually examined the PCA plots for individuals that appeared to be outliers with respect to other individuals with the same population label. For this analysis, following Pickrell et al. [2012], we used only the SNPs ascertained in a single Ju|'hoan (HGDP "San") individual in order to expose the population structure within the southern Africa Khoisan. Shown in each panel are all the individuals removed from analysis (red circles), along with the other individuals from their population (green circles).
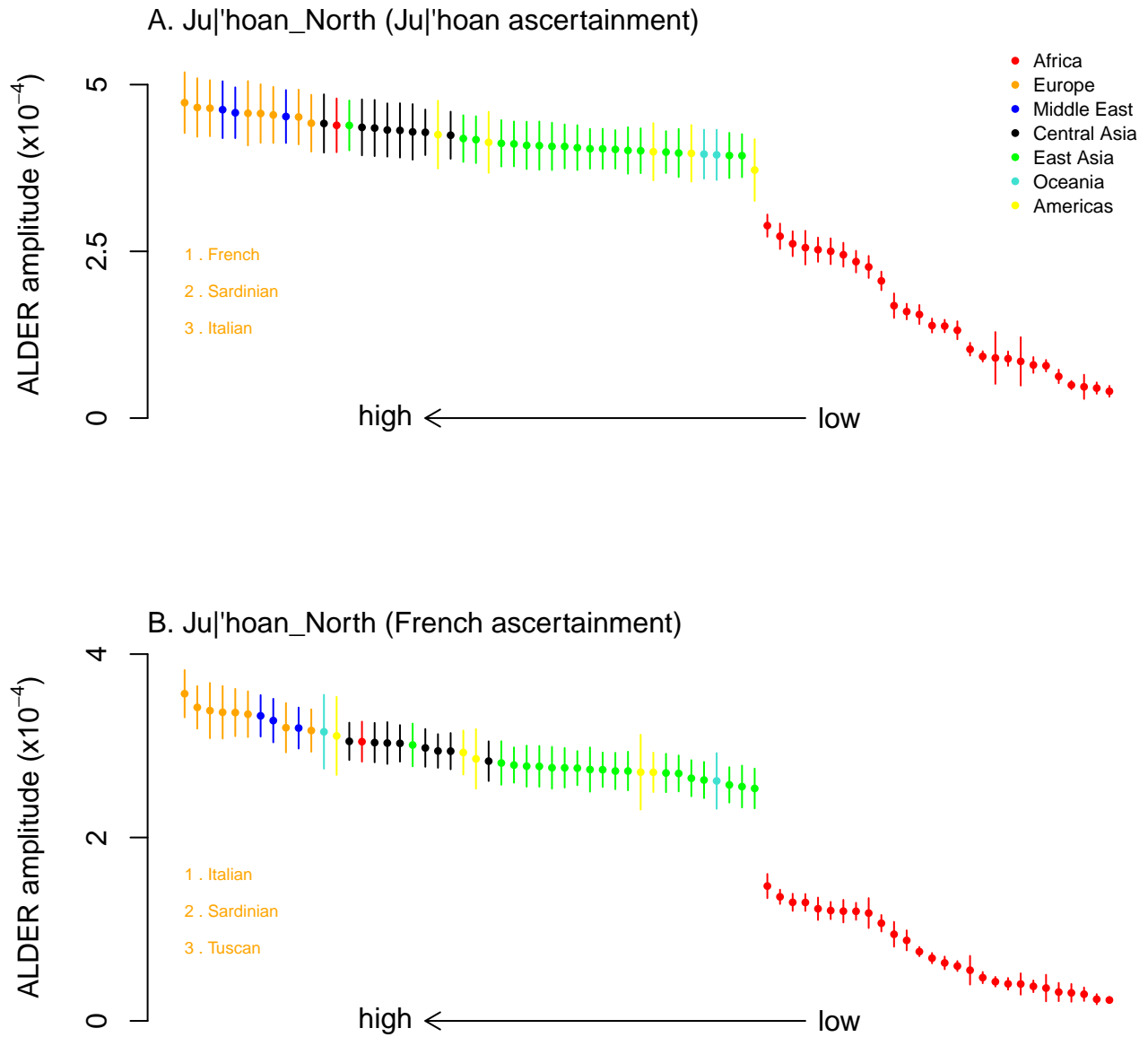
Figure 2: **Signal of west Eurasian ancestry in the Ju|'hoan_North is robust to SNP ascertainment.** This figure is identical to Figure 1 in the main text, except the amplitudes were calculated using only SNPs on the Human Origins Array from individual ascertainment panels.
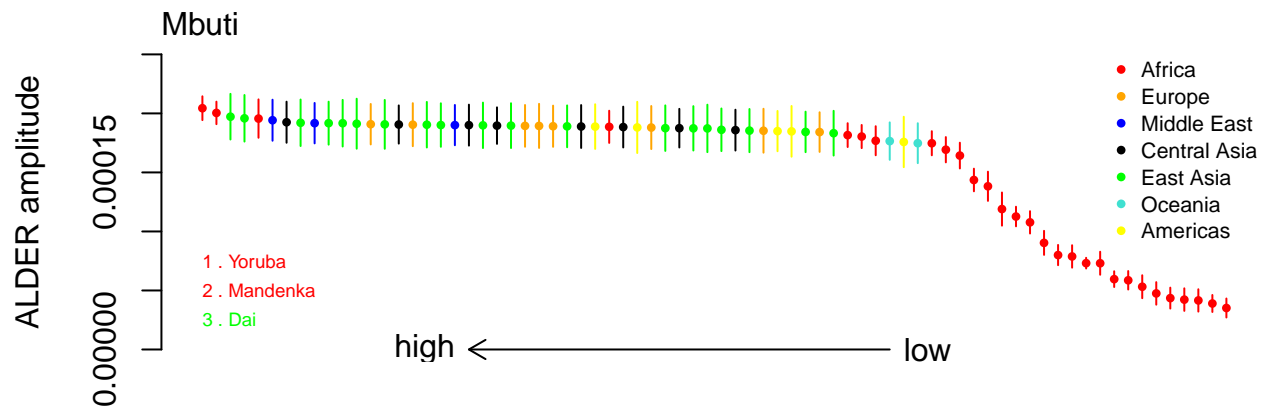
Figure 3: **Identifying sources of admixture in the Mbuti.** We calculated weighted LD curves in the Mbuti, using the Mbuti themselves as one reference population and a set of other worldwide populations as the other reference. As in Figure 1 in the main text, we show the estimated amplitudes of these LD curves, colored according to the continent of the reference population.
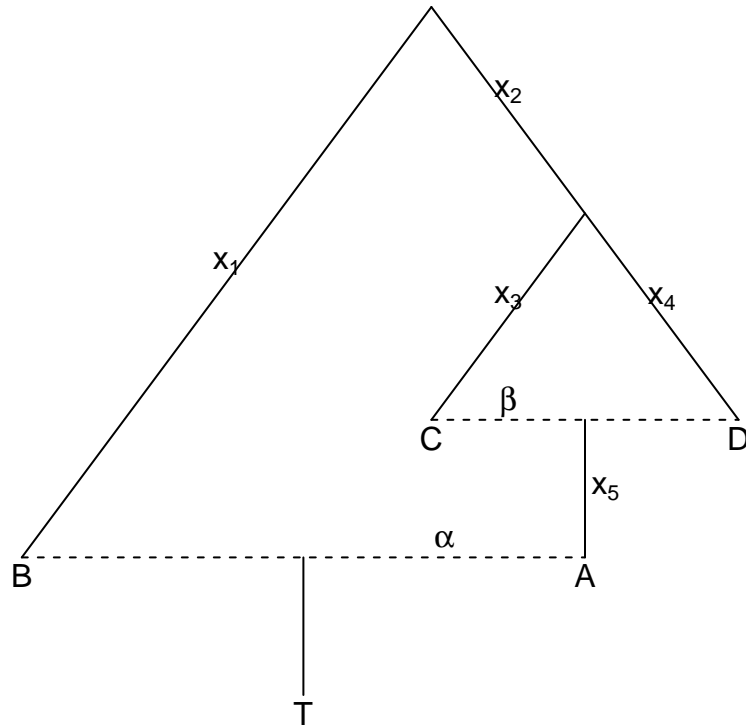
Figure 4: **Schematic of a history with two admixture events.** Shown is an example admixture graph, where solid lines represent population relationships and dotted lines represent admixture events. The capital letters represent populations, α and β represent the admixture proportions in the two mixture events, and the x parameters represent branch lengths in units of genetic drift.
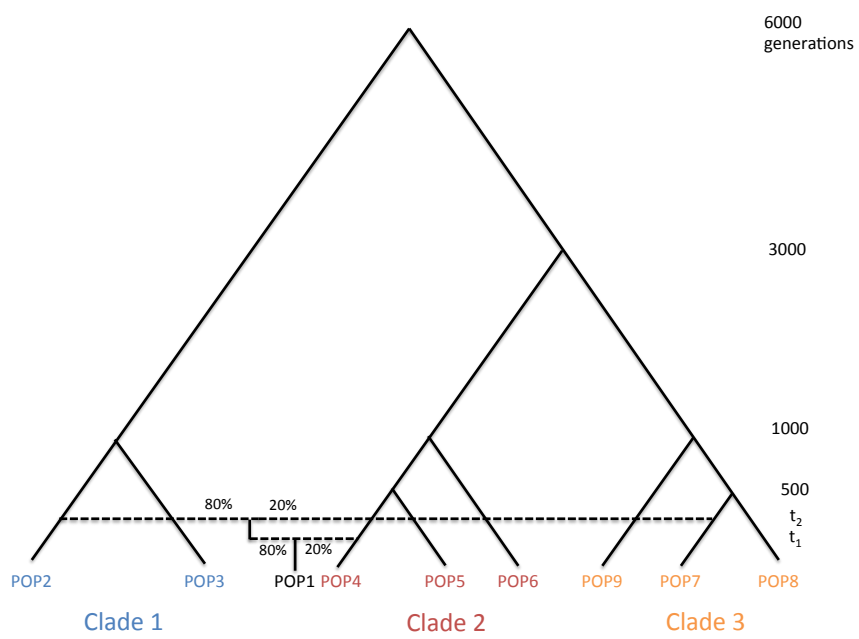
Figure 5: **Population history used in simulations.**
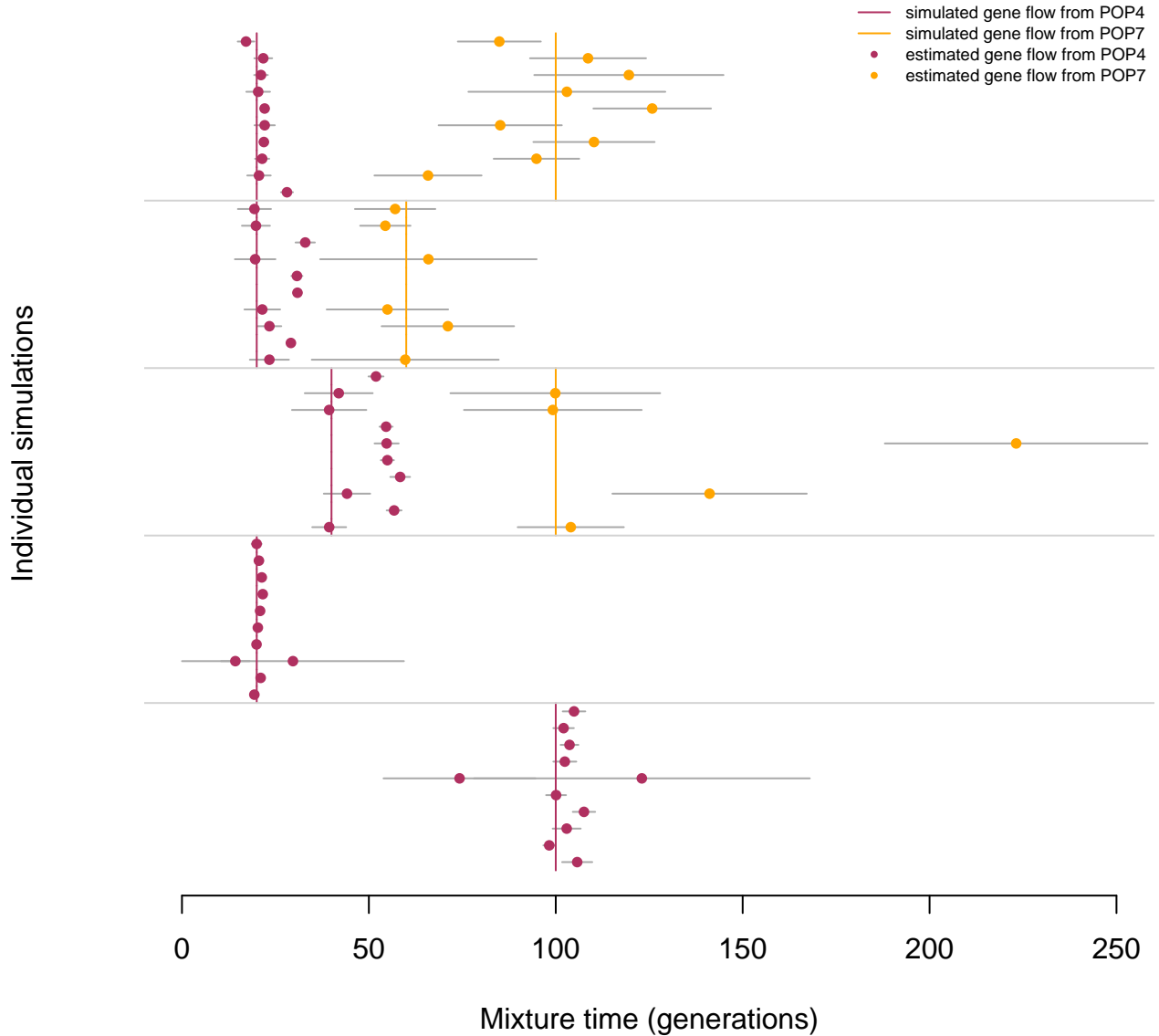
Figure 6: **Simulation results under pulse admixture model.** We tested our method for estimating multiple mixture dates using simulations. In each simulation, we generated data from the demographic model in Supplementary Figure 5 with mixture dates denoted by the colored lines. We then ran our method; each point represents an estimated mixture event, and shown are the within-simulation standard errors. Points are colored according to the inferred source of the admixture. In no simulation did we detect more than two admixture events.
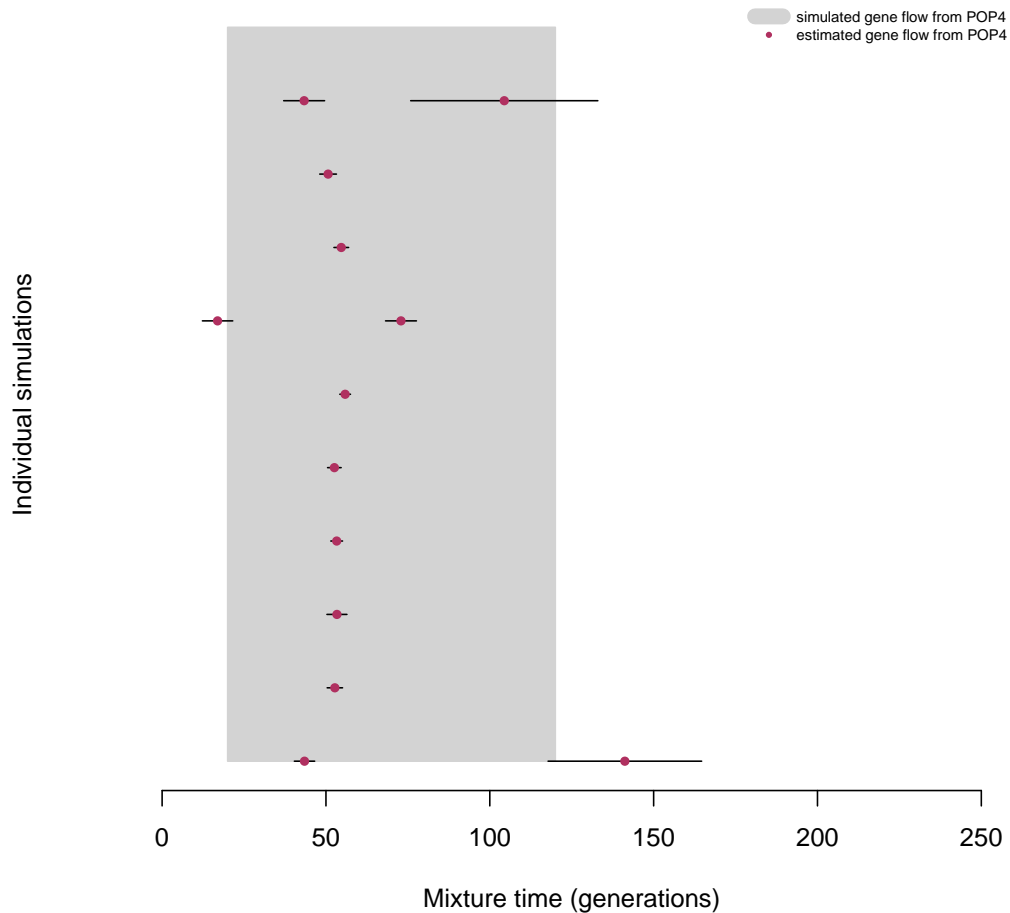
Figure 7: **Simulation results under continuous gene flow model.** We tested our method for estimating multiple mixture dates using simulations. In each simulation, we generated data from the demographic model in Supplementary Figure 5 with only gene flow from POP4. In these simulations, instead of 20% admixture at a single point in time, we simulated 0.2% admixture per generation over 100 generations (for a total of 20% admixture). The grey box shows the 100 generations over which admixture is occurring. We then ran our method; each point represents an inferred mixture event, and shown are the within-simulation standard errors.

Reference populations	Amplitude 1 (x10^{-4})	Amplitude 2 (x10^{-4})
POP2;POP7	0.17	0.084
POP2;POP8	0.16	0.084
POP2;POP9	0.16	0.086
POP2;POP4	0.15	0.1
POP2;POP5	0.15	0.099
POP2;POP4	0.15	0.1
POP2;POP5	0.15	0.099
POP3;POP4	0.14	0.095
POP2;POP6	0.15	0.094
POP3;POP5	0.14	0.092
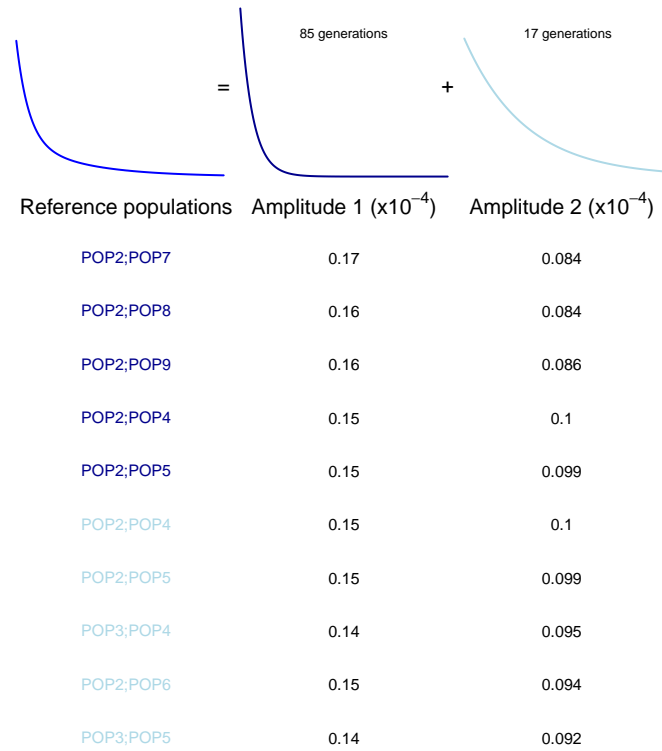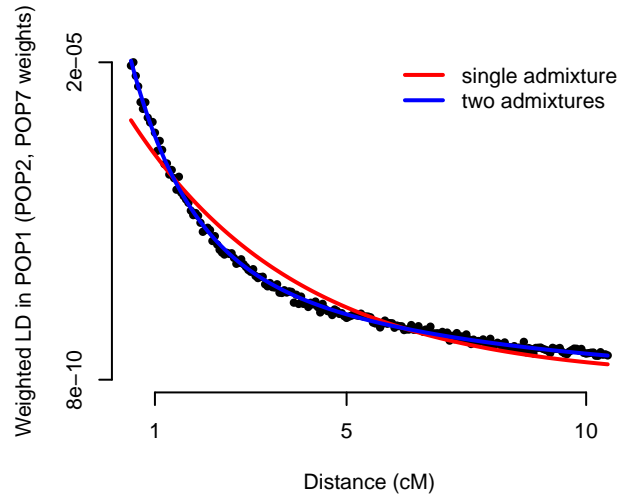
Figure 8: **Example simulation with one recent and one old admixture event.** We simulated data under the demographic model in Supplementary Figure 5, where $t_1 = 20$ and $t_2 = 100$. We then fit a model of multiple mixture events. Shown in red is the fitted model with a single admixture event; in blue is the fitted model with two admixture events. Below the graph are the five population pairs with the largest weights on the first and second inferred admixture events. In both cases the inferred mixing population is the correct one.
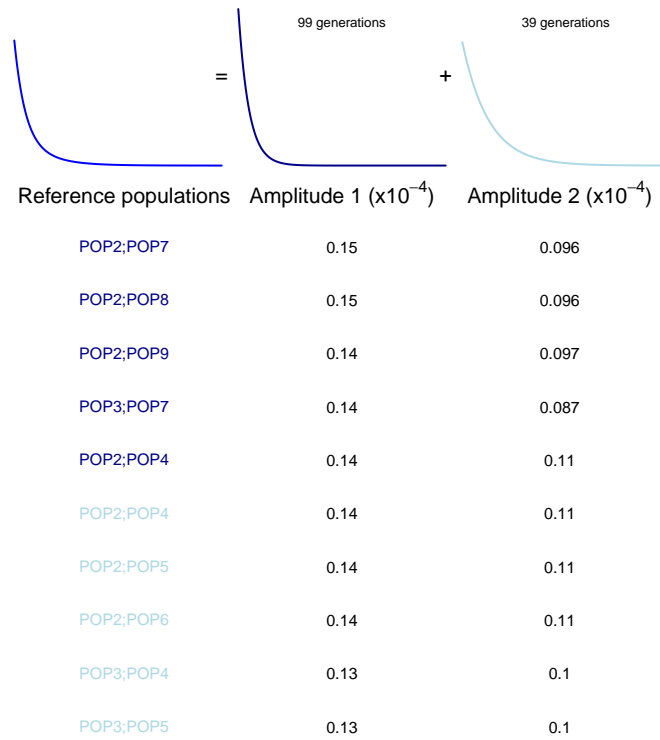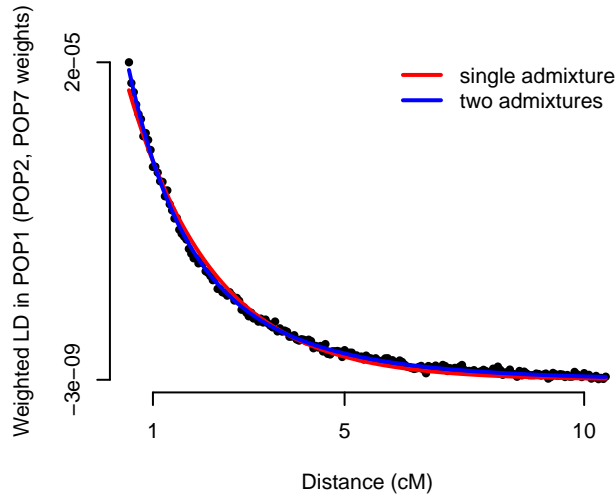
Figure 9: **Example simulation with two old admixture events.** We simulated data under the demographic model in Supplementary Figure 5, where $t_1 = 40$ and $t_2 = 100$. We then fit a model of multiple mixture events. Shown in red is the fitted model with a single admixture event; in blue is the fitted model with two admixture events. Below the graph are the five population pairs with the largest weights on the first and second inferred admixture events. In both cases the inferred mixing population is the correct one.
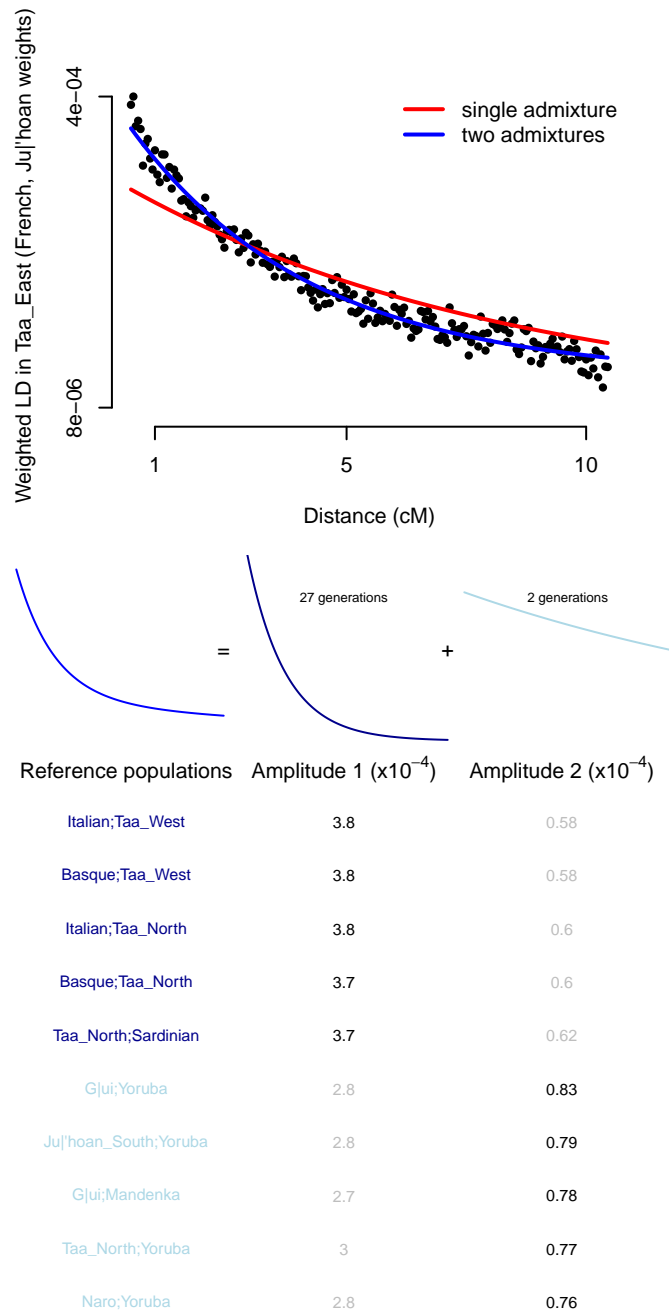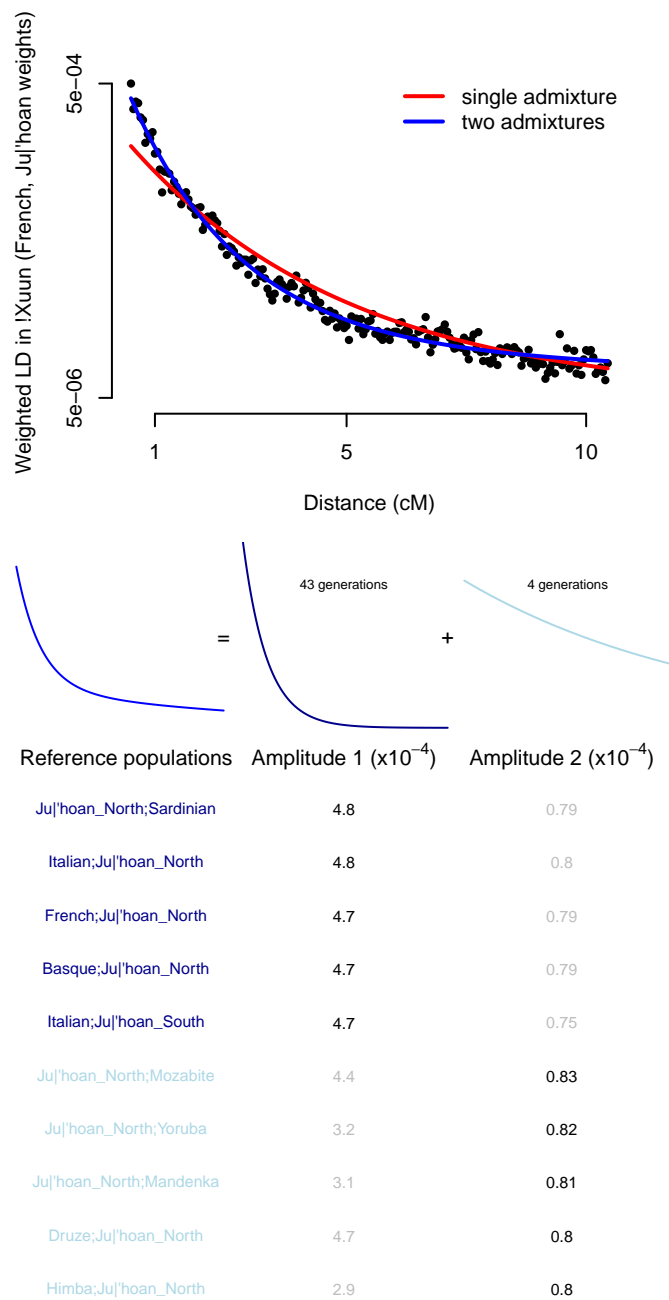
Figure 10**: Fitted admixture model in the Taa_East.** See the caption to Figure 3 in the main text for details.
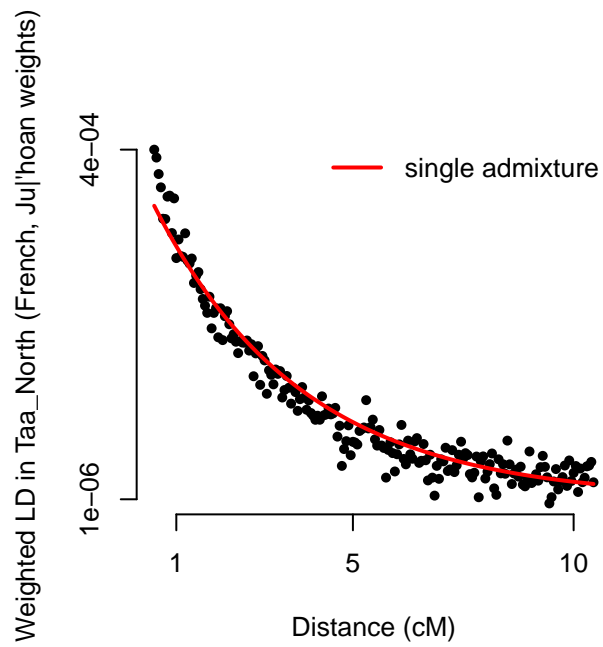
Reference populations	Amplitude 1 (x10^{-4})
Druze;Taa_West	4
Druze;G|ui	3.9
Italian;Taa_West	3.9
G|ui;Italian	3.9
French;Taa_West	3.9
Sardinian;Taa_West	3.9
G|ui;Sardinian	3.9
French;G|ui	3.9
Druze;Naro	3.9
Tuscan;Taa_West	3.8

Figure 11: **Fitted admixture model in the Taa_North.** See the caption to Figure 3 in the main text for details.
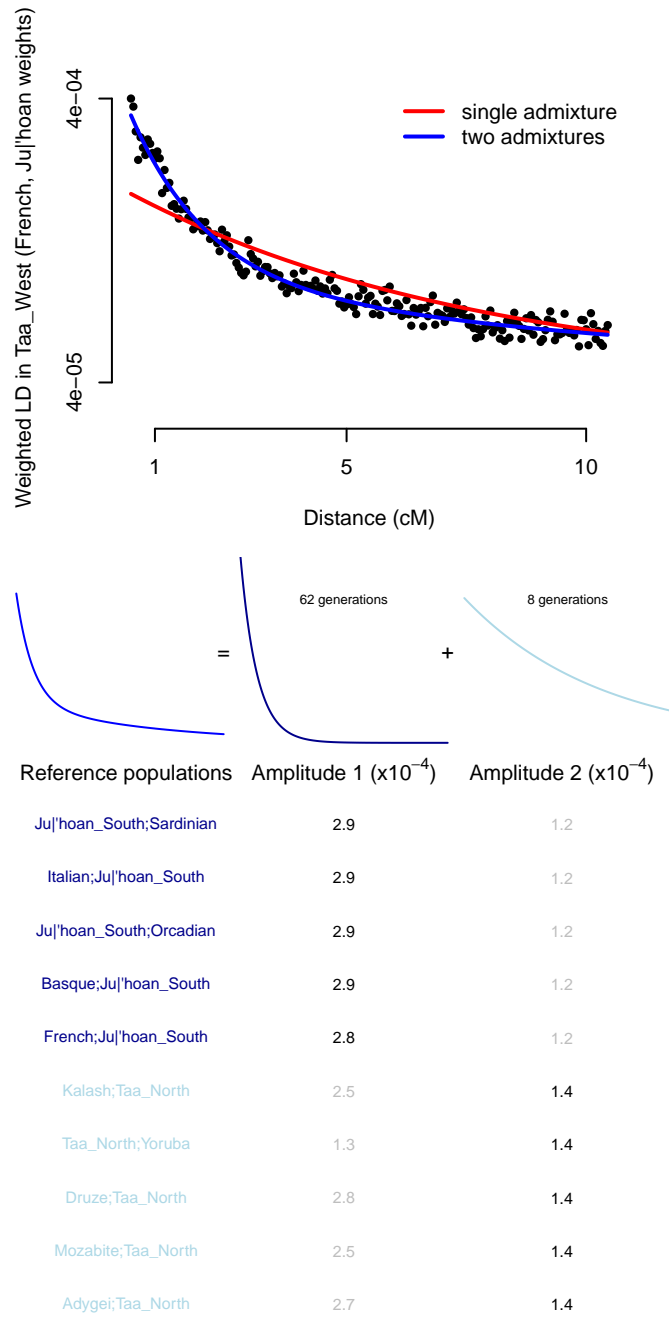
Figure 12: **Fitted admixture model in the Taa_West.** See the caption to Figure 3 in the main text for details.

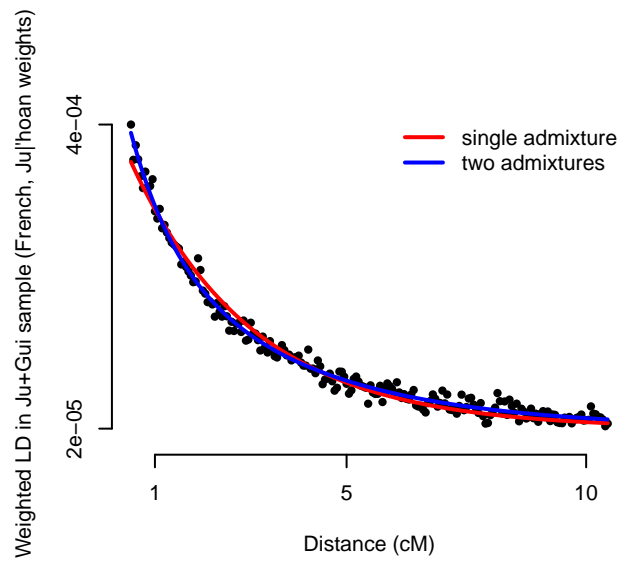Figure 13: **Fitted admixture model in the ǂHoan.** See the caption to Figure 3 in the main text for details.
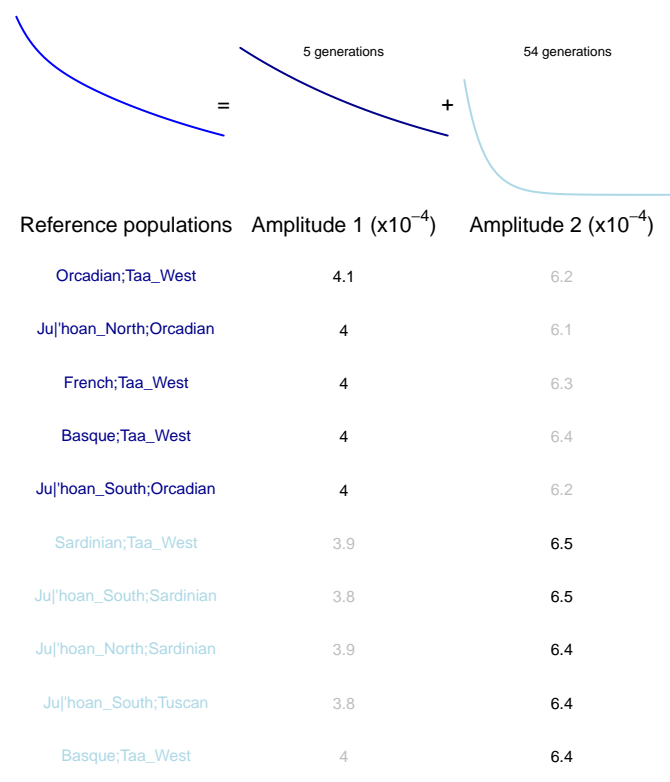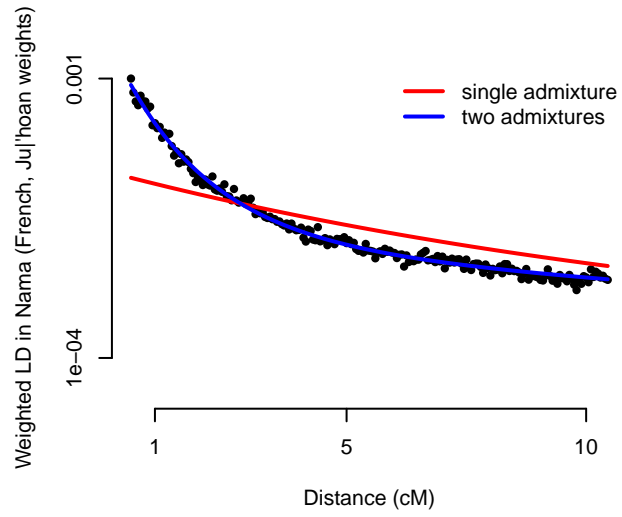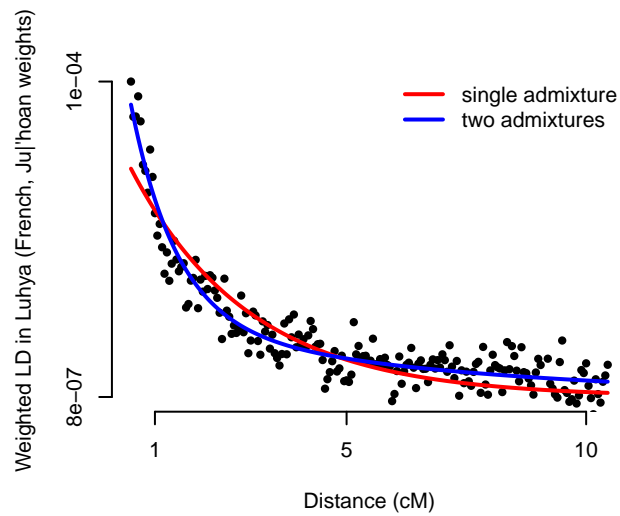
Figure 14: Fitted admixture model in the Nama. See the caption to Figure 3 in the main text for details.

Figure 15: **Fitted admixture model in the Shua.** See the caption to Figure 3 in the main text for details.
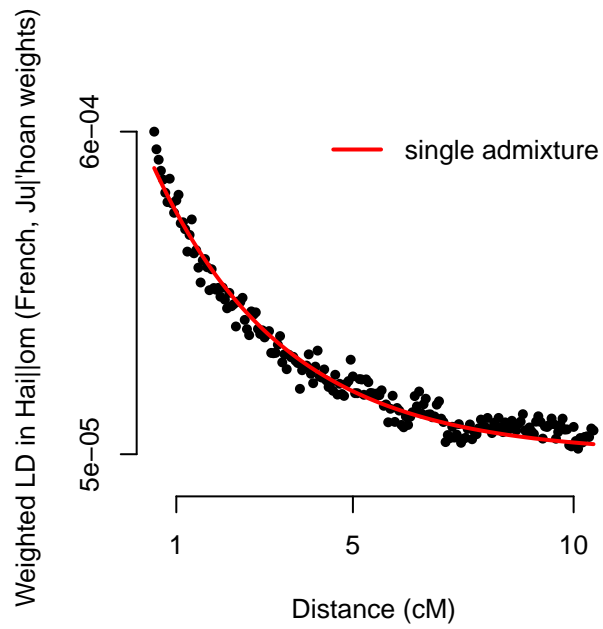
Reference populations	Amplitude 1 (x10^{-4})
Ju|'hoan_North;Sardinian	6.2
Italian;Ju|'hoan_North	6.1
French;Ju|'hoan_North	6
Ju|'hoan_North;Tuscan	6
Druze;Ju|'hoan_North	6
Basque;Ju|'hoan_North	6
Ju|'hoan_South;Sardinian	6
Ju|'hoan_North;Palestinian	5.9
Adygei;Ju|'hoan_North	5.9
Ju|'hoan_North;Orcadian	5.9

Figure 16: **Fitted admixture model in the Hai‖om.** See the caption to Figure 3 in the main text for details.
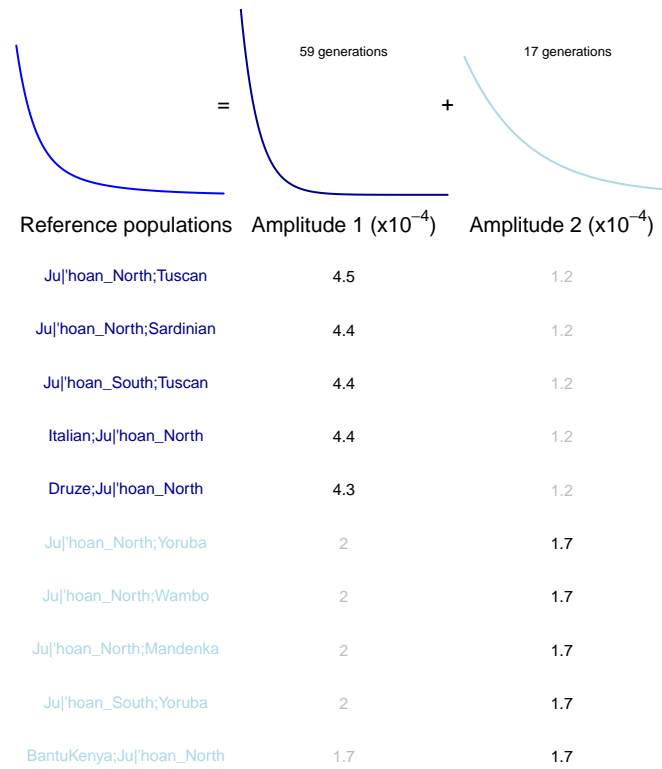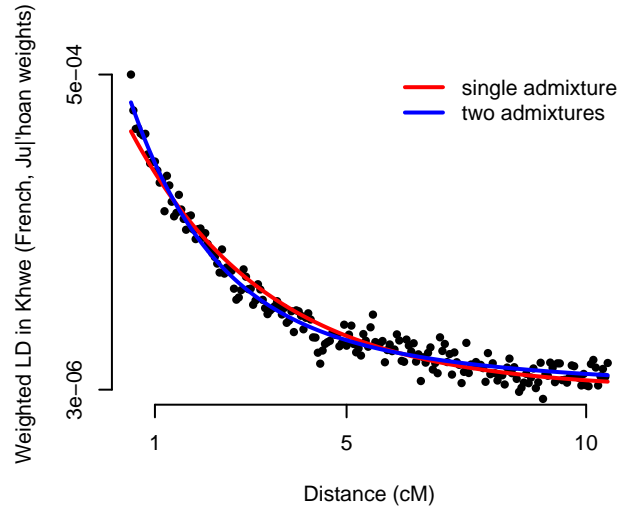
Figure 17: **Fitted admixture model in the Khwe.** See the caption to Figure 3 in the main text for details.
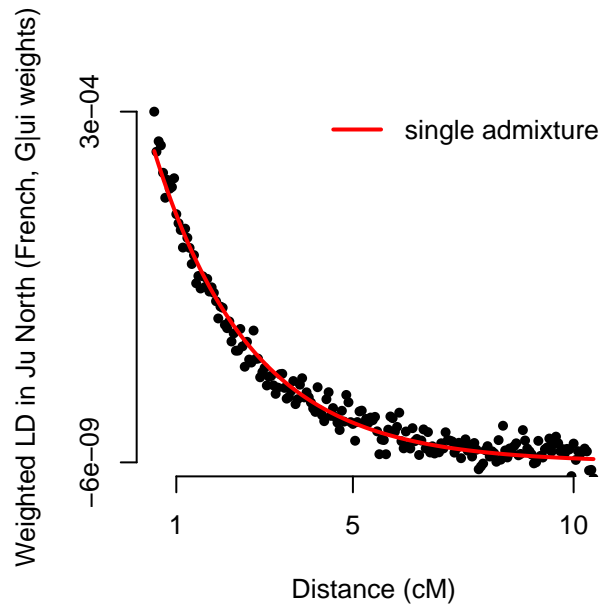
Reference populations	Amplitude 1 (x10^{-4})
Ju|'hoan_South;Sardinian	4.1
Ju|'hoan_South;Orcadian	4.1
Italian;Ju|'hoan_South	4.1
Basque;Ju|'hoan_South	4.1
Ju|'hoan_South;Tuscan	4.1
French;Ju|'hoan_South	4.1
Druze;Ju|'hoan_South	4.1
Adygei;Ju|'hoan_South	4
Bedouin;Ju|'hoan_South	4
Ju|'hoan_South;Russian	4

Figure 18: **Fitted admixture model in the Ju|'hoan_North.** See the caption to Figure 3 in the main text for details.

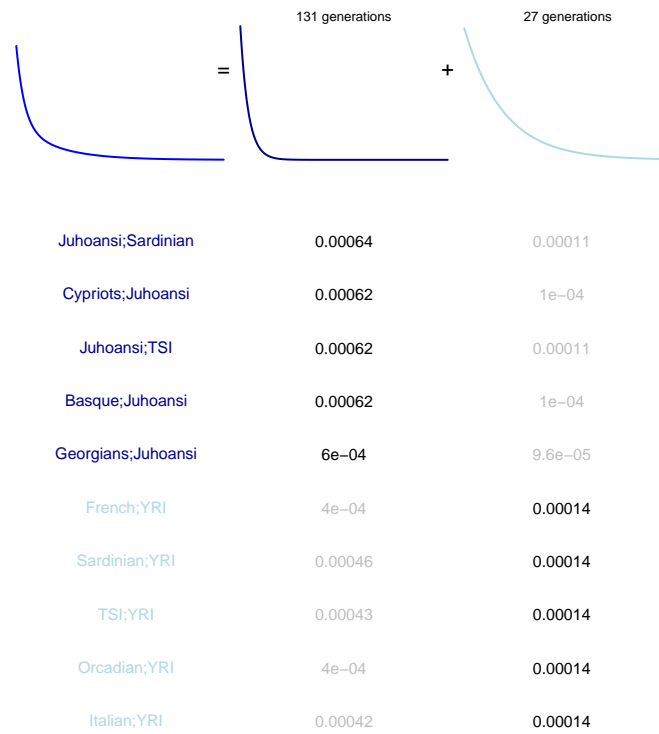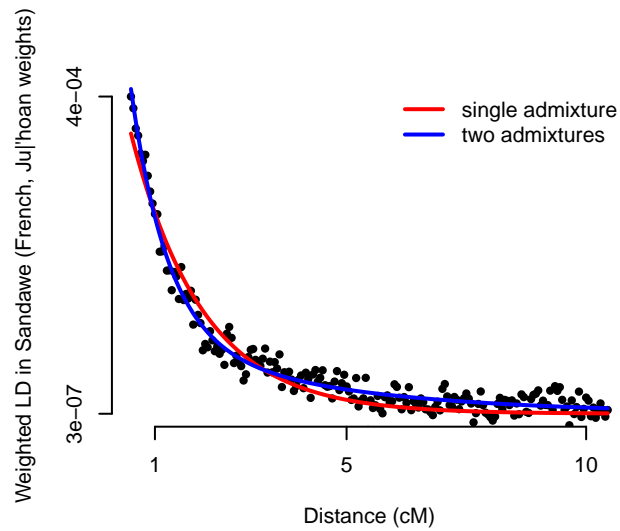Figure 19: **Fitted admixture model in the Naro.** See the caption to Figure 3 in the main text for details.

Figure 20: **Fitted admixture model in the Tshwa.** See the caption to Figure 3 in the main text for details.

Figure 21: **Fitted admixture model in the G|ui.** See the caption to Figure 3 in the main text for details.
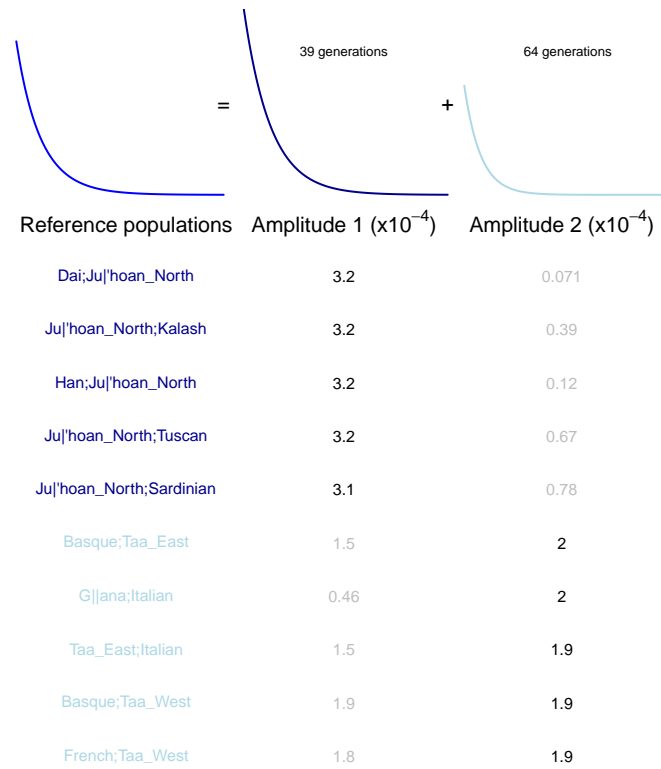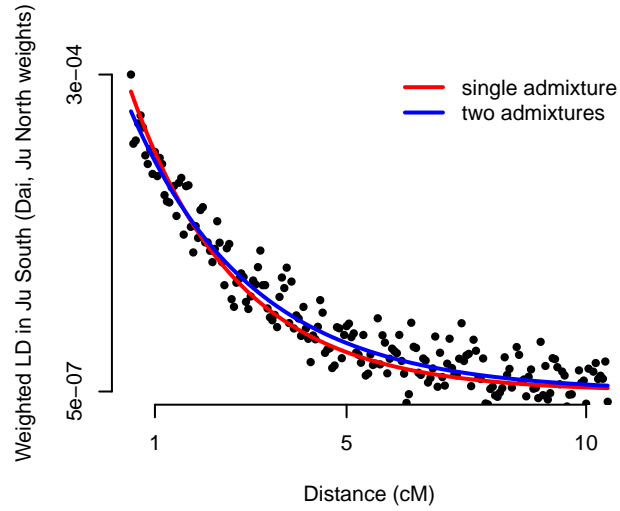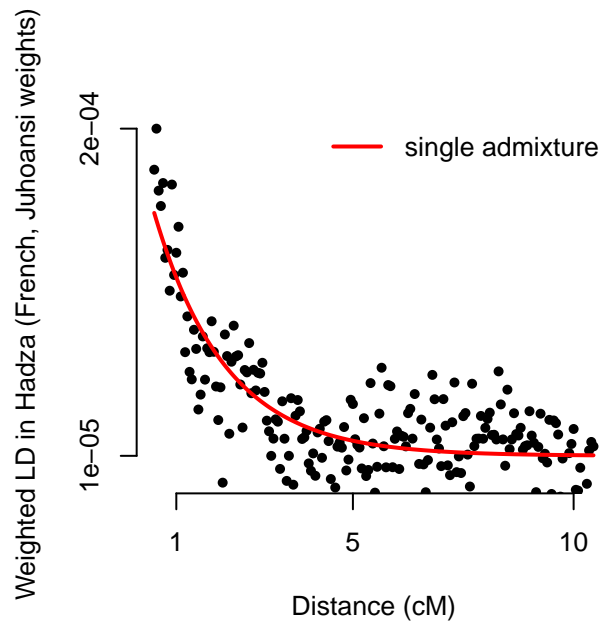
Figure 22: **Fitted admixture model in the Ju|'hoan_South.** See the caption to Figure 3 in the main text for details.

Reference populations	Amplitude 1 (x10^{-4})	Amplitude 2 (x10^{-4})
Ju|'hoan_North;Sardinian	4.8	0.79
Italian;Ju|'hoan_North	4.8	0.8
French;Ju|'hoan_North	4.7	0.79
Basque;Ju|'hoan_North	4.7	0.79
Italian;Ju|'hoan_South	4.7	0.75
Ju|'hoan_North;Mozabite	4.4	0.83
Ju|'hoan_North;Yoruba	3.2	0.82
Ju|'hoan_North;Mandenka	3.1	0.81
Druze;Ju|'hoan_North	4.7	0.8
Himba;Ju|'hoan_North	2.9	0.8

Figure 23: **Fitted admixture model in the !Xuun.** See the caption to Figure 3 in the main text for details.
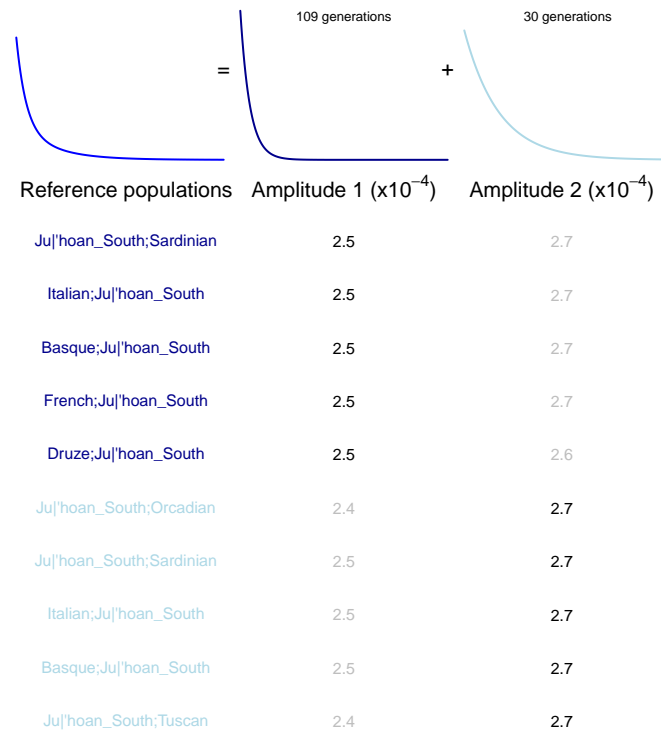
Figure 24: **Fitted admixture model in the combined Ju|'hoan_North and G|ui samples.**
See the caption to Figure 3 in the main text for details.
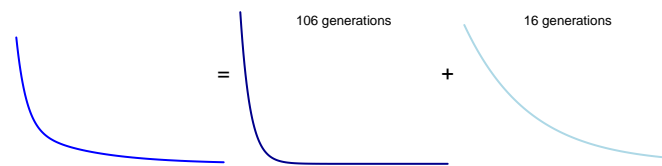
Figure 25: **Fitted admixture model in the Luhya.** See the caption to Figure 3 in the main text for details.
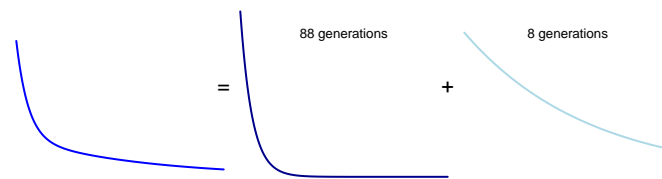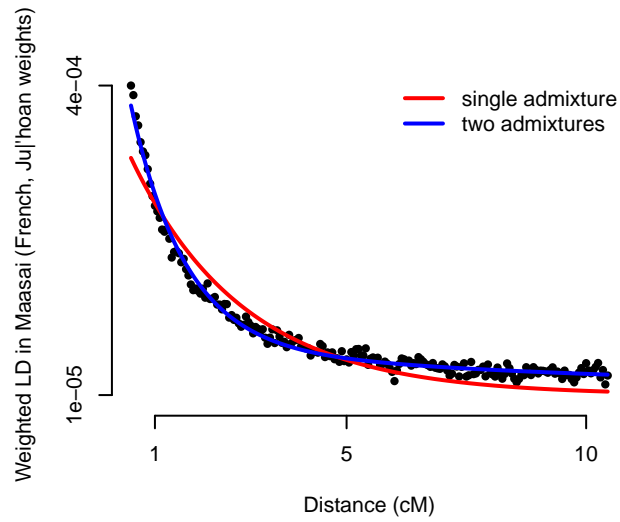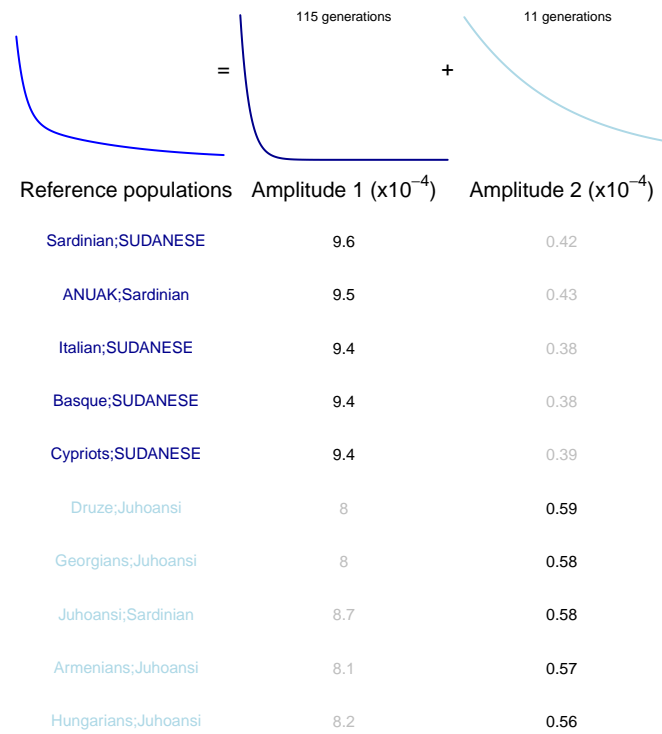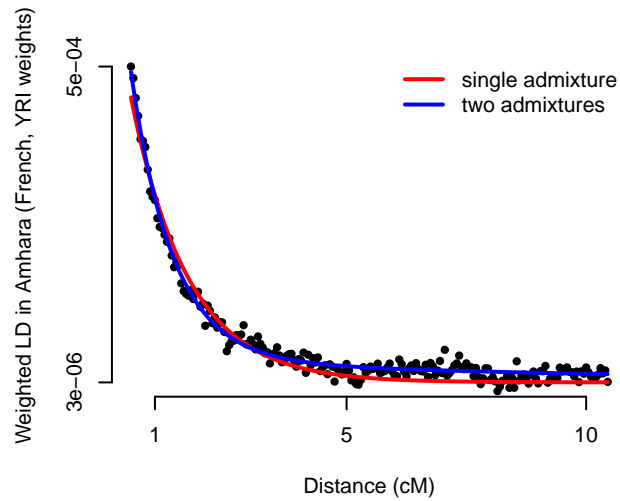
Figure 26: **Fitted admixture model in the Maasai.** See the caption to Figure 3 in the main text for details.

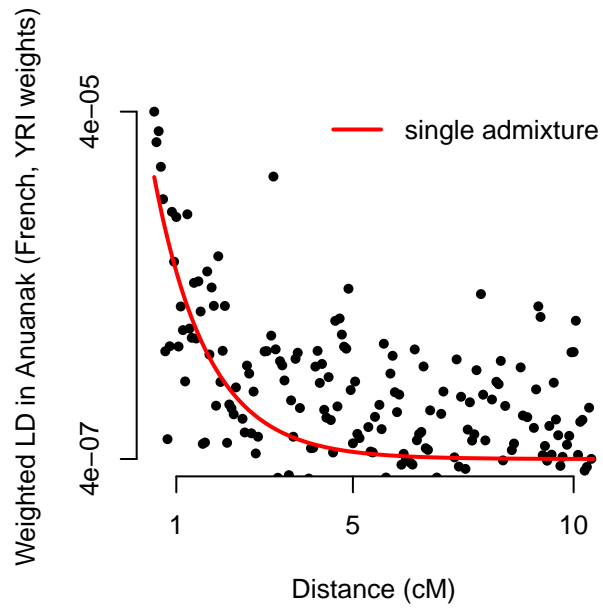Figure 27: **Fitted admixture model in the Sandawe.** See the caption to Figure 3 in the main text for details.

Figure 28: **Fitted admixture model in the Hadza.** See the caption to Figure 3 in the main text for details.
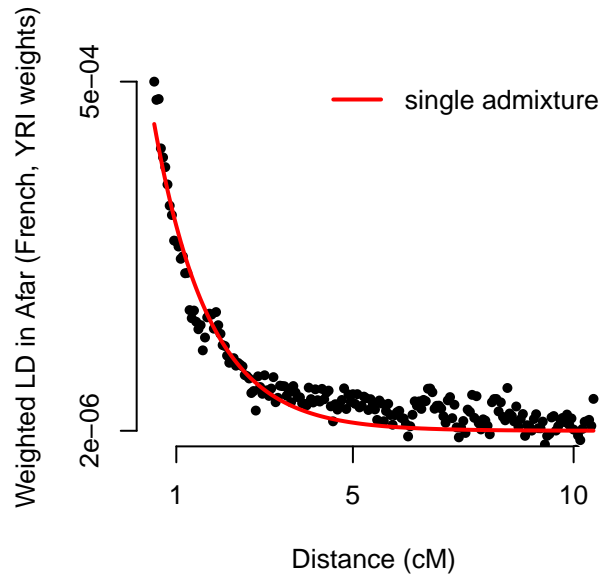
Reference populations	Amplitude 1 (x10^{-4})
Sardinian;SUDANESE	7.9
Italian;SUDANESE	7.8
SUDANESE;TSI	7.8
ANUAK;Sardinian	7.7
Orcadian;SUDANESE	7.7
French;SUDANESE	7.7
Cypriots;SUDANESE	7.7
ANUAK;Italian	7.7
ANUAK;TSI	7.6
CEU;SUDANESE	7.6

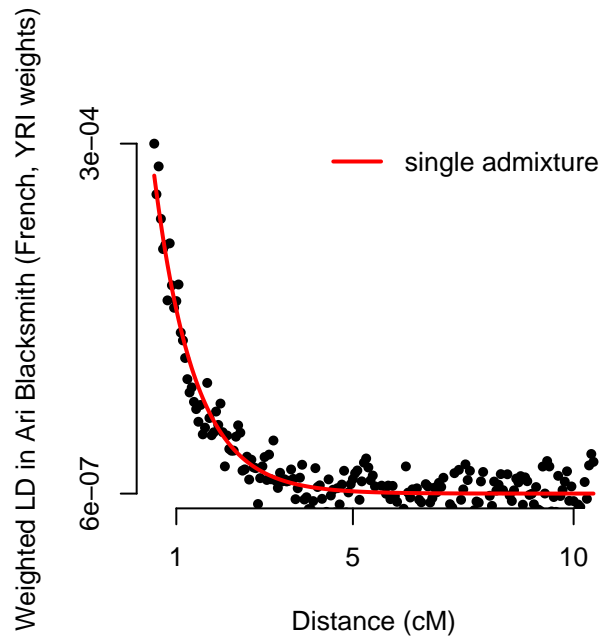Figure 29: **Fitted admixture model in the Afar.** See the caption to Figure 3 in the main text for details.

Figure 30**: Fitted admixture model in the Amhara.** See the caption to Figure 3 in the main text for details.

Figure 31: **Fitted admixture model in the Anuak.** See the caption to Figure 3 in the main text for details.

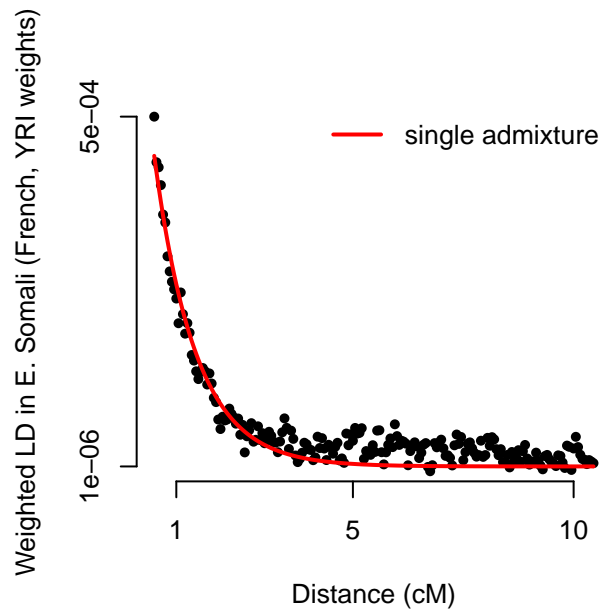| Reference populations	Amplitude 1 (x10⁻⁴)
MbutiPygmy;Sardinian	5.2
Juhoansi;Sardinian	5.1
Basque;MbutiPygmy	5.1
MbutiPygmy;TSI	5
Italian;MbutiPygmy	5
Cypriots;MbutiPygmy	5
Juhoansi;TSI	5
Basque;Juhoansi	5
BiakaPygmy;Sardinian	5
French;MbutiPygmy	4.9

Figure 32: **Fitted admixture model in the Ari Blacksmiths.** See the caption to Figure 3 in the main text for details.

Figure 33: **Fitted admixture model in the Ari Cultivators.** See the caption to Figure 3 in the main text for details.

Reference populations	Amplitude 1 (x10^{-4})
ANUAK;Sardinian	8
Sardinian;SUDANESE	8
ANUAK;Italian	7.9
Italian;SUDANESE	7.9
ANUAK;TSI	7.9
SUDANESE;TSI	7.8
ANUAK;Basque	7.8
Basque;SUDANESE	7.8
BiakaPygmy;Sardinian	7.8
MbutiPygmy;Sardinian	7.8

Figure 34: **Fitted admixture model in the Ethiopian Somali.** See the caption to Figure 3 in the main text for details.
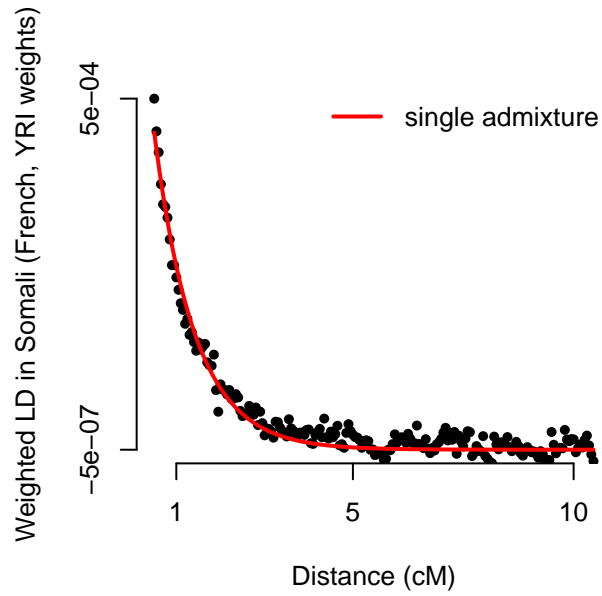
Reference populations	Amplitude 1 (x10^{-4})
Sardinian;SUDANESE	8.6
ANUAK;Sardinian	8.5
Italian;SUDANESE	8.5
SUDANESE;TSI	8.4
ANUAK;Italian	8.4
Cypriots;SUDANESE	8.4
Basque;SUDANESE	8.4
ANUAK;TSI	8.3
French;SUDANESE	8.3
MbutiPygmy;Sardinian	8.3

Figure 35: **Fitted admixture model in the Somali.** See the caption to Figure 3 in the main text for details.

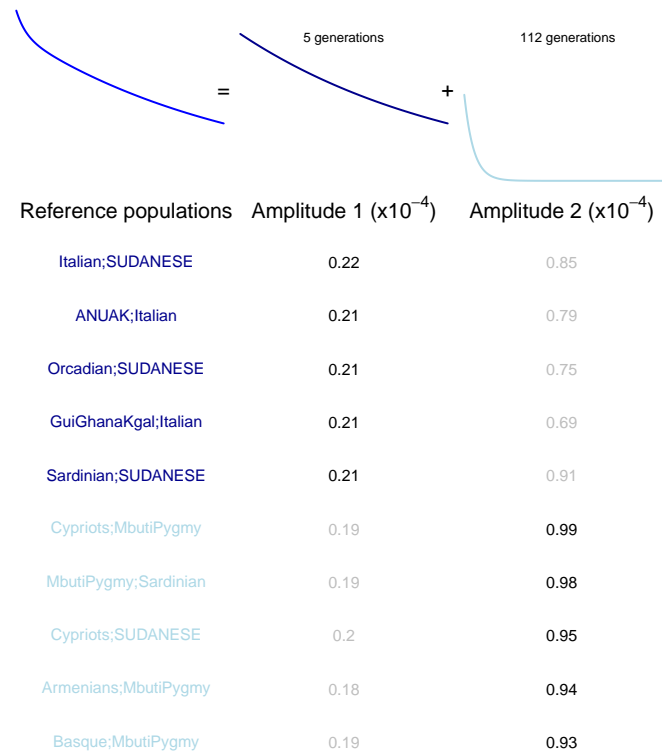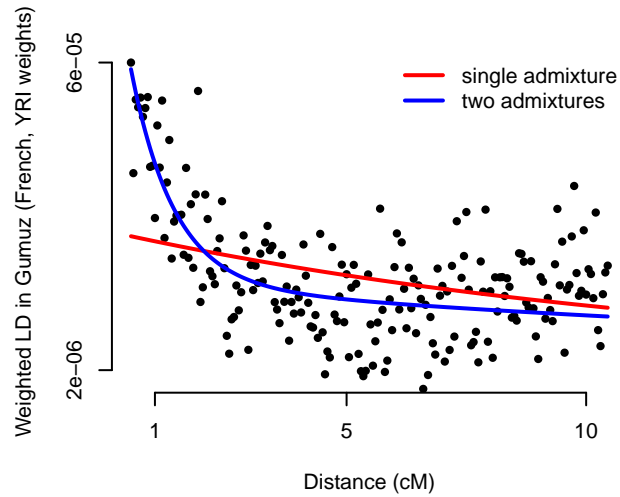| Reference populations	Amplitude 1 ($\times 10^{-4}$)	Amplitude 2 ($\times 10^{-4}$)
Italian;SUDANESE	0.22	0.85
ANUAK;Italian	0.21	0.79
Orcadian;SUDANESE	0.21	0.75
GuiGhanaKgal;Italian	0.21	0.69
Sardinian;SUDANESE	0.21	0.91
Cypriots;MbutiPygmy	0.19	0.99
MbutiPygmy;Sardinian	0.19	0.98
Cypriots;SUDANESE	0.2	0.95
Armenians;MbutiPygmy	0.18	0.94
Basque;MbutiPygmy	0.19	0.93

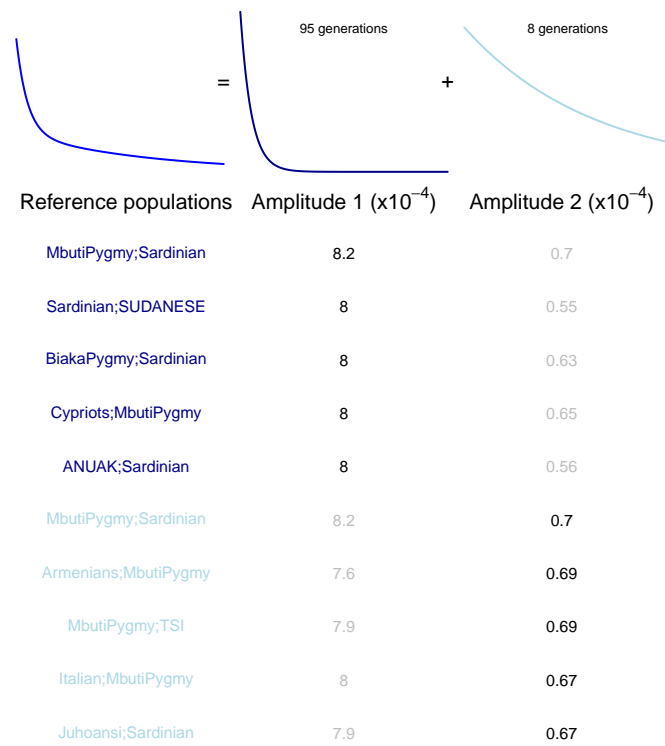Figure 36: **Fitted admixture model in the Gumuz.** See the caption to Figure 3 in the main text for details.

Figure 37: **Fitted admixture model in the Oromo.** See the caption to Figure 3 in the main text for details.
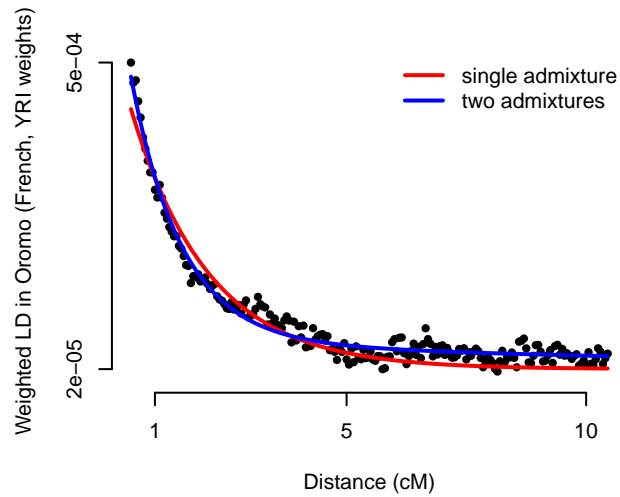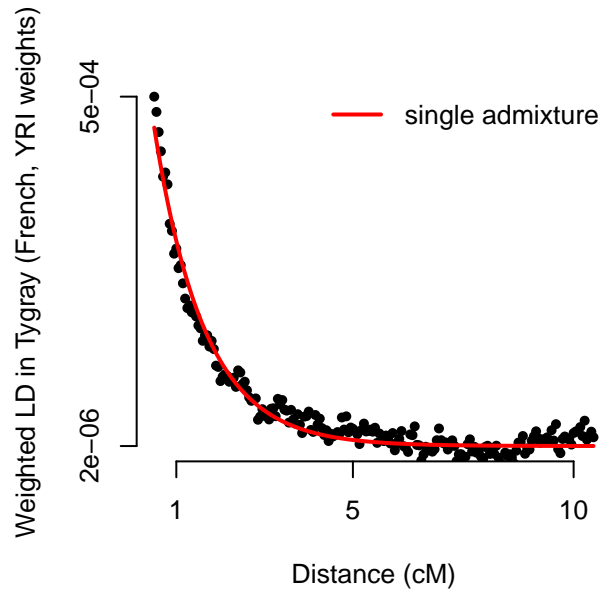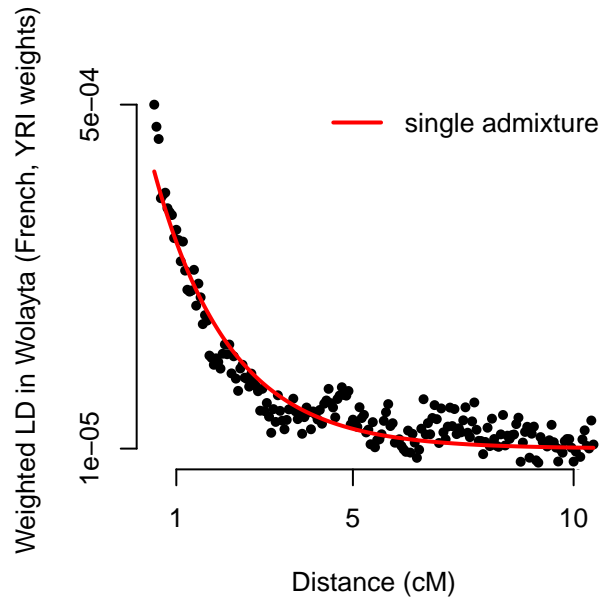
Figure 38: **Fitted admixture model in the Tygray.** See the caption to Figure 3 in the main text for details.

Reference populations	Amplitude 1 (x10^{-4})
Sardinian;SUDANESE	8.7
ANUAK;Sardinian	8.7
Cypriots;SUDANESE	8.7
ANUAK;Cypriots	8.6
MbutiPygmy;Sardinian	8.6
Italian;SUDANESE	8.6
ANUAK;Italian	8.5
SUDANESE;TSI	8.5
ANUAK;TSI	8.5
Cypriots;MbutiPygmy	8.5

Reference populations	Amplitude 1 (x10^{-4})
Cypriots;Juhoansi	6.5
Juhoansi;Sardinian	6.5
MbutiPygmy;Sardinian	6.5
Italian;Juhoansi	6.5
Cypriots;MbutiPygmy	6.5
Italian;MbutiPygmy	6.4
Juhoansi;TSI	6.4
MbutiPygmy;TSI	6.3
Armenians;Juhoansi	6.3
French;Juhoansi	6.3

Figure 39: **Fitted admixture model in the Wolayta.** See the caption to Figure 3 in the main text for details.
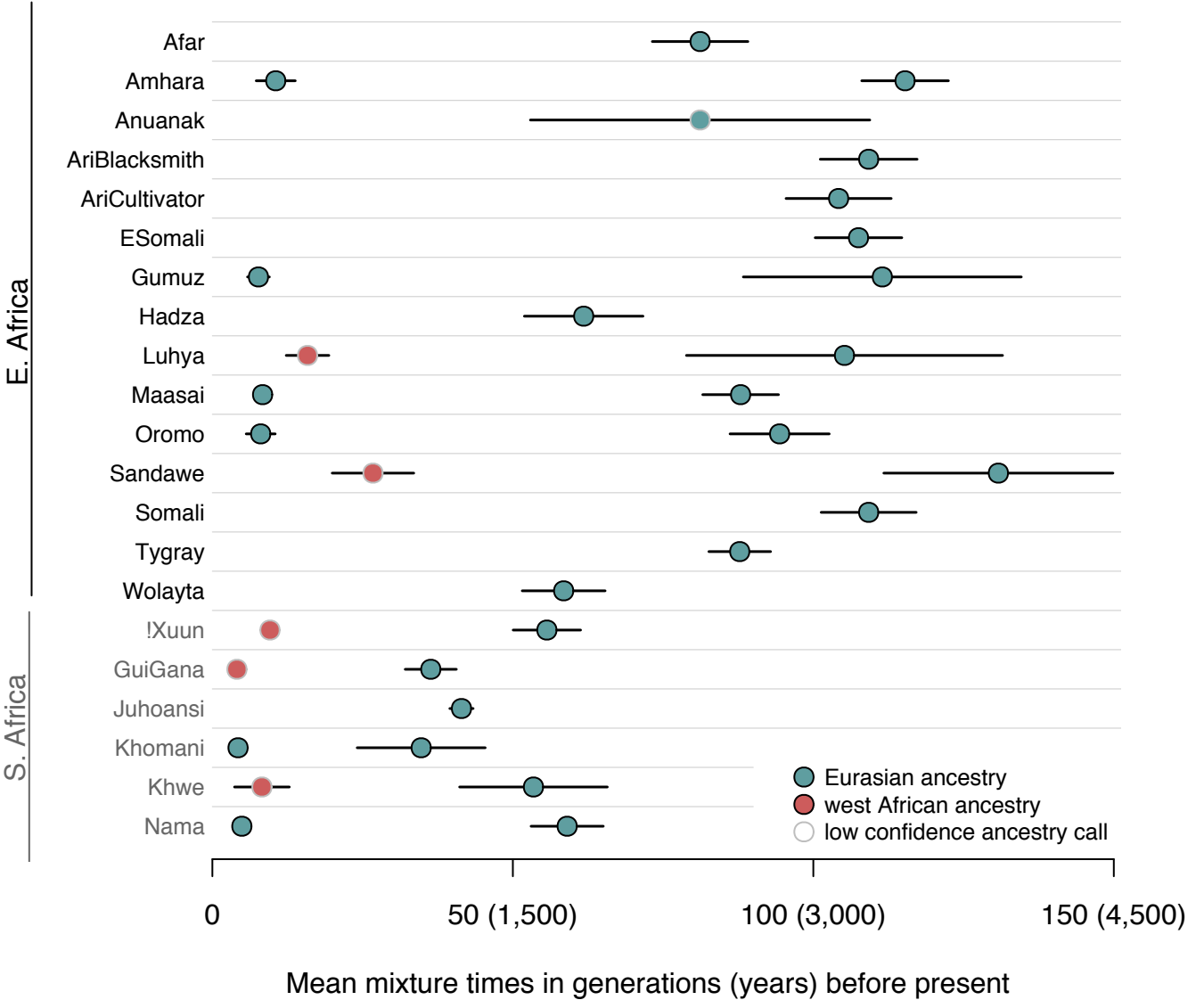
Figure 40: **Inferred times of admixture in southern and eastern Africa.** We applied our method to estimate the number of mixture events in the history of a population and their times; plotted are the estimated times. Lines represent a single standard error. The eastern African populations are the same as those in Figure 4 in the main text, while the southern African populations are those from Schlebusch et al. [2012]. In this figure the estimates in the southern and eastern African populations come from the exact same set of SNPs.
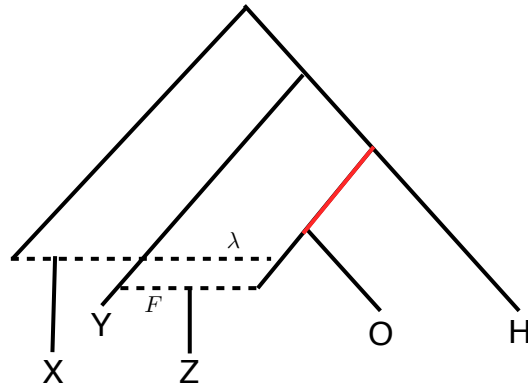
Figure 41: **Assumed population phylogeny for f_4 estimation of west Eurasian ancestry in African populations.** To calculate the proportion of west Eurasian ancestry in each southern and eastern African population, we used the following phylogeny for the Khoisan populations. X represents the test population, Y represents the Yoruba, Z represents either the Druze, O represents the Orcadians, H represents the Han, λ represents the proportions of west Eurasian ancestry in X, and F represents the proportion of Yoruba-like ancestry in Z. The red branch is the relevant one for estimating west Eurasian ancestry. If we let l be the length of the red branch, $f_4(H, O; X, Z) = (1-\lambda-F)l$, and $f_4(H, O; Y, Z) = (1-F)l$. Thus, the f_4 ratio $\frac{f_4(H,O;X,Z)}{f_4(H,O;Y,Z)} = \frac{1-\lambda-F}{1-F}$.

References

Altshuler, D., Gibbs, R., Peltonen, L., Dermitzakis, E., Schaffner, S., Yu, F., Bonnen, P., de Bakker, P., Deloukas, P., Gabriel, S., *et al.*, 2010. Integrating common and rare genetic variation in diverse human populations. *Nature*, **467**(7311):52.

Behar, D. M., Yunusbayev, B., Metspalu, M., Metspalu, E., Rosset, S., Parik, J., Rootsi, S., Chaubey, G., Kutuev, I., Yudkovsky, G., *et al.*, 2010. The genome-wide structure of the Jewish people. *Nature*, **466**(7303):238–42.

Chakraborty, R. and Weiss, K. M., 1988. Admixture as a tool for finding linked genes and detecting that difference from allelic association between loci. *Proc Natl Acad Sci U S A*, **85**(23):9119–23.

Chen, G. K., Marjoram, P., and Wall, J. D., 2009. Fast and flexible simulation of DNA sequence data. *Genome Res*, **19**(1):136–42.

Galassi, M., Davies, J., Theiler, J., Gough, B., Jungman, G., Alken, P., Booth, M., and Rossi, F., 2002. *GNU scientific library*.

Haber, M., Gauguier, D., Youhanna, S., Patterson, N., Moorjani, P., Botigué, L. R., Platt, D. E., Matisoo-Smith, E., Soria-Hernanz, D. F., Wells, R. S., *et al.*, 2013. Genome-wide diversity in the levant reveals recent structuring by culture. *PLoS Genet*, **9**(2):e1003316.

Henn, B. M., Gignoux, C. R., Jobin, M., Granka, J. M., Macpherson, J. M., Kidd, J. M., Rodríguez-Botigué, L., Ramachandran, S., Hon, L., Brisbin, A., *et al.*, 2011. Hunter-gatherer genomic diversity suggests a southern African origin for modern humans. *Proc Natl Acad Sci U S A*, **108**(13):5154–62.

Li, J. Z., Absher, D. M., Tang, H., Southwick, A. M., Casto, A. M., Ramachandran, S., Cann, H. M., Barsh, G. S., Feldman, M., Cavalli-Sforza, L. L., *et al.*, 2008. Worldwide human relationships inferred from genome-wide patterns of variation. *Science*, **319**(5866):1100–1104.

Loh, P.-R., Lipson, M., Patterson, N., Moorjani, P., Pickrell, J. K., Reich, D., and Berger, B., 2013. Inferring admixture histories of human populations using linkage disequilibrium. *Genetics*, **193**(4):1233–54.

Meyer, M., Kircher, M., Gansauge, M.-T., Li, H., Racimo, F., Mallick, S., Schraiber, J. G., Jay, F., Prüfer, K., de Filippo, C., *et al.*, 2012. A high-coverage genome sequence from an archaic Denisovan individual. *Science*, **338**(6104):222–6.

Moorjani, P., Patterson, N., Hirschhorn, J. N., Keinan, A., Hao, L., Atzmon, G., Burns, E., Ostrer, H., Price, A. L., and Reich, D., *et al.*, 2011. The history of African gene flow into Southern Europeans, Levantines, and Jews. *PLoS Genet*, **7**(4):e1001373.

Pagani, L., Kivisild, T., Tarekegn, A., Ekong, R., Plaster, C., Gallego Romero, I., Ayub, Q., Mehdi, S. Q., Thomas, M. G., Luiselli, D., *et al.*, 2012. Ethiopian genetic diversity reveals linguistic stratification and complex influences on the Ethiopian gene pool. *Am J Hum Genet*, **91**(1):83–96.

Patterson, N., Moorjani, P., Luo, Y., Mallick, S., Rohland, N., Zhan, Y., Genschoreck, T., Webster, T., and Reich, D., 2012. Ancient admixture in human history. *Genetics*, **192**(3):1065–93.

Patterson, N., Petersen, D. C., van der Ross, R. E., Sudoyo, H., Glashoff, R. H., Marzuki, S., Reich, D., and Hayes, V. M., 2010. Genetic structure of a unique admixed population: implications for medical research. *Hum Mol Genet*, **19**(3):411–9.

Patterson, N., Price, A. L., and Reich, D., 2006. Population structure and eigenanalysis. *PLoS Genet*, **2**(12):e190.

Pickrell, J. K., Patterson, N., Barbieri, C., Berthold, F., Gerlach, L., Güldemann, T., Kure, B., Mpoloka, S. W., Nakagawa, H., Naumann, C., *et al.*, 2012. The genetic prehistory of southern Africa. *Nat Commun*, **3**:1143.

R Development Core Team, 2011. *R: A Language and Environment for Statistical Computing*. R Foundation for Statistical Computing, Vienna, Austria. ISBN 3-900051-07-0.

Schlebusch, C. M., Skoglund, P., Sjödin, P., Gattepaille, L. M., Hernandez, D., Jay, F., Li, S., De Jongh, M., Singleton, A., Blum, M. G. B., *et al.*, 2012. Genomic variation in seven Khoe-San groups reveals adaptation and complex African history. *Science*, **338**(6105):374–9.